

Copyright Warning & Restrictions

The copyright law of the United States (Title 17, United States Code) governs the making of photocopies or other reproductions of copyrighted material.

Under certain conditions specified in the law, libraries and archives are authorized to furnish a photocopy or other reproduction. One of these specified conditions is that the photocopy or reproduction is not to be “used for any purpose other than private study, scholarship, or research.” If a user makes a request for, or later uses, a photocopy or reproduction for purposes in excess of “fair use” that user may be liable for copyright infringement,

This institution reserves the right to refuse to accept a copying order if, in its judgment, fulfillment of the order would involve violation of copyright law.

Please Note: The author retains the copyright while the New Jersey Institute of Technology reserves the right to distribute this thesis or dissertation

Printing note: If you do not wish to print this page, then select “Pages from: first page # to: last page #” on the print dialog screen

The Van Houten library has removed some of the personal information and all signatures from the approval page and biographical sketches of theses and dissertations in order to protect the identity of NJIT graduates and faculty.

ABSTRACT

REMEDICATION OF CONTAMINATED SITES USING HOT GAS INJECTION

by

Sanjay Jayabal

Remediation of contaminated subsurface sites at lower cost and time than currently used technologies are being demonstrated for a systems concept using new technology developed at the Hazardous Substance Management Research Center at New Jersey Institute of Technology. A technique for pneumatic fracture is employed to "open" subsurface passages to enhance vacuum extraction of contaminants. Economical and environmentally sound destruction of these contaminants is then accomplished using catalytic oxidation followed by scrubbing to remove air pollutants. The hot gas from this phase of the process is then injected into the subsurface formation after being used to preheat the fuel/air mixture to catalyst operating temperature, to increase contaminant temperature, hence vapor pressure leading to increased contaminant mass removal rates.

A computer based model of the subsurface heating process has been developed to provide for engineering design. Using the heat injection well as the radial center for a cylindrical coordinate system, a non-steady state numerical heat transfer model is utilized to predict ground temperature in three dimensions assuming uniform gas flow along the fracture planes.

Extension of the above model has been made to include contaminant mass removal. The change in rate of evaporation of chlorocarbon contaminants and low vapor pressure organic liquids in the vadose zone is related to the computed temperature increases.

This connection allows assessment of the expected change in the measured mass removal rates of contaminants as a result of hot gas injection into the sub-surface.

It was found that trichloroethylene (TCE) is removed from the surface of the formation cracks at gas temperatures of 635 °F and redeposits further downstream as the temperature drops to 60 °F. If the formation is heated for a sufficiently long time then the TCE would be transported to the extraction well. For accurate predictions of temperature distribution and mass removal rates, the model must be calibrated on the actual site of the clean-up.

**REMEDICATION OF CONTAMINATED SITES
USING HOT GAS INJECTION**

by
Sanjay Jayabal

**A Thesis
Submitted to the Faculty of
New Jersey Institute of Technology
in Partial Fulfillment of the Requirements for the Degree of
Master of Science in Mechanical Engineering**

Department of Mechanical and Industrial Engineering

May 1994

APPROVAL PAGE

REMEDICATION OF CONTAMINATED SITES
USING HOT GAS INJECTION

Sanjay Jayabal

Dr. Henry Shaw, Thesis Advisor
Professor of Chemical Engineering, NJIT

_____ Date

Dr. Rong Yaw Chen, Committee Member
Associate Graduate Chairperson and Professor
of Mechanical Engineering, NJIT

_____ Date

Dr. John G. Stevens, Committee Member
Professor of Mathematics, Montclair State College

_____ Date

BIOGRAPHICAL SKETCH

Author: Sanjay Jayabal

Degree: Master of Science in Mechanical Engineering

Date: January 1994

Undergraduate Education and Graduate Education:

- Master of Science in Mechanical Engineering,
New Jersey Institute of Technology, Newark, NJ, 1994
- Bachelor of Engineering in Mechanical Engineering,
PSG College of Technology, Coimbatore, India, 1990

Major: Mechanical Engineering

Presentations and Publications:

Jayabal, Sanjay. "Remediation of Contaminated Sites using Hot Gas Injection." *ASME Student Technical Conference*. Polytechnic University, Brooklyn, NY.

This thesis is dedicated to my parents

ACKNOWLEDGMENT

The author wishes to express his sincere gratitude to his advisor, Professor Henry Shaw, for his guidance, friendship, and moral support throughout this research.

The author would also like to deeply express his indebtedness to Late Dr. Anthony E. Cerkanowicz for providing the opportunity to work on this research project, provide funding throughout, and to have imparted a lot of knowledge and insight on the research work.

Special thanks to Professor Rong Yaw Chen for serving as a member of the committee.

The author would like to convey his sincere thanks to Professor John Stevens of Montclair State College for his timely help in altering the program code and his total involvement in this research work by offering pertinent suggestions and making it a success.

The author highly appreciates and is very grateful to Professor Richard Cole of Stevens Institute of Technology for his interest in this work and his invaluable time and suggestions.

TABLE OF CONTENTS

Chapter	Page
1 INTRODUCTION	1
1.1 Overview	1
1.2 Description of Component Processes	1
1.2.1 Pneumatic Fracturing	1
1.2.1.1 Fracture Dimensions	2
1.2.2 Catalytic Oxidation	6
1.2.2.1 Catalytic Destruction of Trichloroethylene	6
1.2.3 HCL Removal & Heat Injection	9
1.3 Objective	10
2 HOT GAS INJECTION MODEL DESCRIPTION	11
2.1 Consolidated Model Description	11
2.1.1 Process Description	11
2.1.2 Mathematical Model Description	13
2.2 Modeling Rationale	14
2.2.1 Heat Transfer Considerations	14
2.2.2 Mass Transport Considerations	17
2.2.3 Technical Rationale	22
2.3 Equations	23
2.4 Integration of Heat and Mass Transport	27
3 TEST CASES	28
3.1 Heat Transfer Iterations	28
3.2 Mass Transport Iterations	30

TABLE OF CONTENTS
(Continued)

Chapter	Page
4 DISCUSSION OF RESULTS	32
4.1 Heat Transfer and Temperature Distribution	32
4.2 Mass Transport and Mass Residual Distribution	36
5 MODEL VERIFICATION	39
6 SUMMARY AND CONCLUSIONS	41
7 RECOMMENDATIONS	43
APPENDIX-A PROGRAM CODE	45
APPENDIX-B DERIVATION OF EQUATIONS	71
APPENDIX-C PHYSICAL PROPERTIES OF CONTAMINANTS	78
APPENDIX-D TRIAL RUN RESULTS	80
REFERENCES	90

LIST OF FIGURES

Figure	Page
1 Pneumatic Fracturing Concept Fine-Grained Soils	3
2 Pneumatic Aeration Concept Coarse-Grained Soils	4
3 Pneumatic Fracturing Concept Rock Formations	5
4 Well Schematic	7
5 Pneumatic Fracturing Injector/Packers	8
6 Pneumatic Fracture-Hot Gas Injection Site Remediation Process Streams	12
7 Subsurface Heat Transfer-Nodal Network	16
8 Subsurface Heating By HGI-24 Hr. Test	29
9 Fracture Temperature-100 SCFM Flue Gas at 700 F Temperature vs Distance from Well	33
10 Fracture Temperature-100 SCFM Flue Gas at 700 F Temperature vs Time	34
11 Rock Temperature-100 SCFM Flue Gas at 700 F 24 Hr. Injection	35
12 TCE at Surface at Different Times and Nodes	37
13 Mass Fraction of Contaminant in Gas for Different Times and Nodes	38
14 Flow Pattern Modification	43

LIST OF TABLES

Table	Page
1 Important Properties of Commonly Occuring Contaminants	78
2 Antoine Constants for Vapor Pressures	79

LIST OF NOMENCLATURE

SYMBOL	DEFINITION	UNITS	
		CUSTOMARY	SI
A_s	Fracture Surface Area	ft ²	m ²
C_p	Specific Heat Capacity	Btu/lb _m °F	kJ/kg.K
D_{ab}	Diffusion Coefficient	ft ² /hr	m ² /s
g_i	Mass Transfer Coefficient	lb _m /ft ² hr	kg/m ² s
h	Heat Transfer Coefficient	Btu/ft ² hr°F	W/m ² .K
h_{fg}	Heat of Vaporization	Btu/lb _m	kJ/kg
K	Thermal Conductivity	Btu/ft hr°F	W/m.K
M_a	Molar Mass of Air	lb _m	kg
M_b	Molar Mass of Contaminant	lb _m	kg
m_i	Mass Flow Rate	lb _m /ft ² hr	kg/m ² s
P_i	Vapor pressure	psia	kPa
q_a	Gas flow rate	ft ³ /hr	m ³ /s
q_s	Convection Heat Flow	Btu/ft ² hr	W/m ²
R	Radial Distance	ft	m
r_w	Radius of well	ft	m
ρ	Density	lb _m /ft ³	kg/m ³
σ_{ab}	Collision Diameter	Å	nm
T	Temperature of gas	°F	K
TT	Solid temperature	°F	K
t	Time	hr	s
V_i	Volume of <i>i</i> th cell	ft ³	m ³
Z	Axial Distance	ft	m

DIMENSIONLESS GROUPS

SYMBOL	DEFINITION
Nu	Nusselt Number
Ω_d	Collision Integral for Diffusion
Pr	Prandtl Number
Re	Reynolds Number
Sc	Schmidt Number
Sh	Sherwood Number

ABBREVIATIONS

HGI	Hot Gas Injection
MFE	Surface Mass Fraction of TCE
MFG	Gas Phase Mass Fraction of TCE
PFE	Pneumatic Fracturing Extraction
TCE	Trichloroethylene
ppm(w)	Parts per Million by Weight
SITE	Superfund Innovative Technology Evaluation
SCFM	Standard Cubic Feet per Minute
HSMRC	Hazardous Substance Management Research Center
VOC	Volatile Organic Compound
ppm(v)	Parts per Million by Volume
psia	Pounds per Square Inch Absolute Pressure.

CHAPTER 1

INTRODUCTION

1.1 Overview

In modeling HGI, a non-steady state process, it is important to understand the component processes that are occurring and affecting it. The following sections describe the other processes required for the entire model. These sections have been included only to illustrate the component processes and give an adequate background to the reader about the whole remediation process. All material covered under the following sections are strictly based on literature survey and deals with developments in these areas.

1.2 Description of Component Processes

1.2.1 Pneumatic Fracturing

Pneumatic fracturing is an in-situ process which enhances the removal and treatment of hazardous organic contaminants from the vadose zone. Its purpose is to reduce treatment time of contaminated formations, and extend available technologies to more difficult geologic conditions. Research activities performed to date have focused on field demonstration of the pneumatic fracturing process, as well as extension of laboratory and theoretical studies. The results of these studies clearly demonstrate that pneumatic fracturing is a viable technology for in-situ remediation of the vadose zone.

The pneumatic fracturing process consists of injecting high pressure air or other gas into contaminated geologic formations at controlled flow rates and pressures, i.e., at a rate that exceeds both the permeability of the formation and the in-situ stresses present. This fractures the medium and creates conductive channels radiating from the injection point. These fractures increase formation permeability and expose more

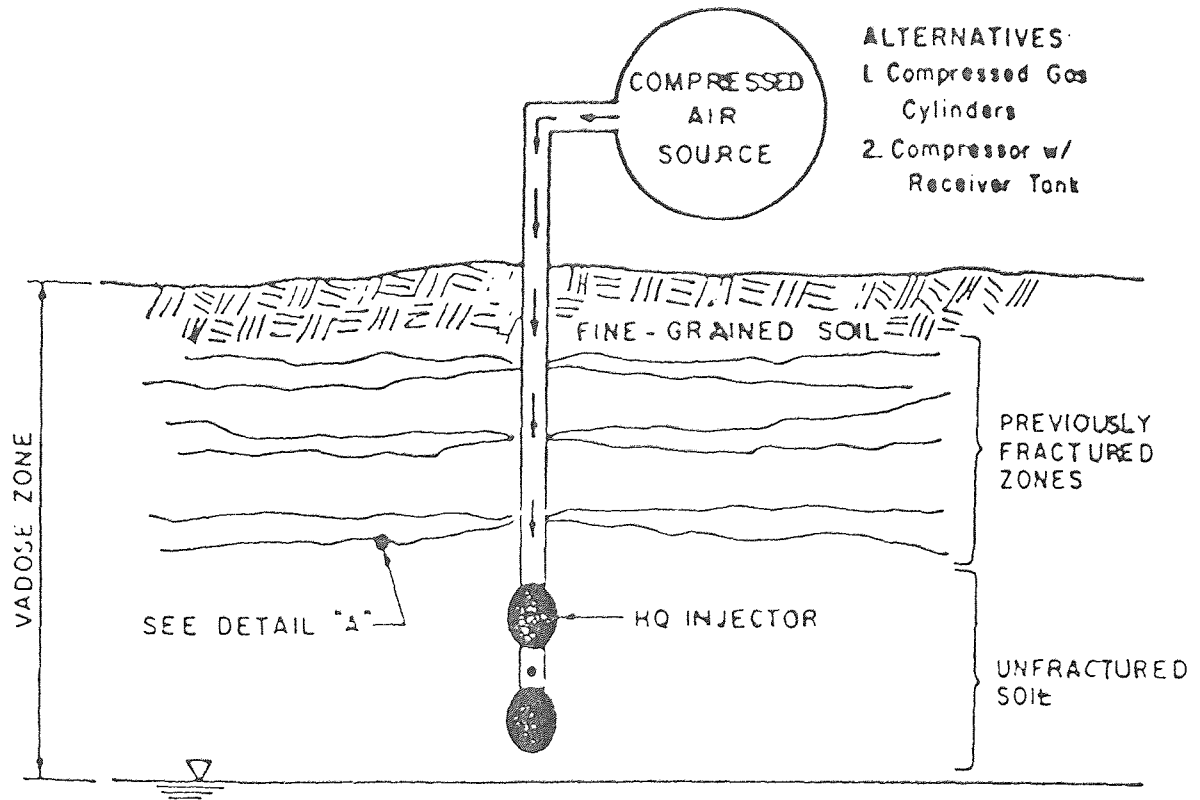
surface area, thereby accelerating removal and/or treatment of contaminants. In summary, pneumatic fracturing transforms contaminant transport from diffusion control before fracturing to convection and diffusion control after fracturing. Figure 1.1 shows that in fine-grained soils, such as silts and clays, pneumatic fracturing increases permeability of the formation. In coarse-grained soils, the process provides a means for rapidly aerating the formation as indicated in Figure 1.2. Figure 1.3 shows that in sedimentary rock formations, the process can widen the aperture of existing discontinuities and clear away soil filling the joints. Pneumatic fracturing can be integrated with a number of in-situ technologies including vapor extraction, bioremediation, and thermal treatment. Further, experiments have shown that fractured soils display 100% to 360% higher removal rates than unfractured soils (Schuring et al., 1991/92).

Theoretical studies of pneumatic fracturing have focused on: (1) the mechanism of pneumatic fracturing; and (2) flow and transport through fractured media. The former has already been explained. In fractured flow studies, analysis of field data has indicated that pneumatically fractured formations conform with the cubic law, i.e., the flow rate through the fractures is proportional to the cube of the fracture aperture. This result emphasizes the high flow potential for even small fractures.(Schuring et al. 1991/92).

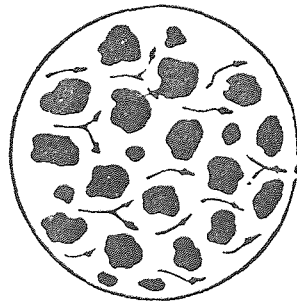
1.2.1.1 Fracture Dimensions

Dimensions of the pneumatic fractures were estimated using ground surface heave. Since soil is a deformable medium, the observed surface heave represents the lower limit of fracture aperture (vertical thickness) and fracture radius.

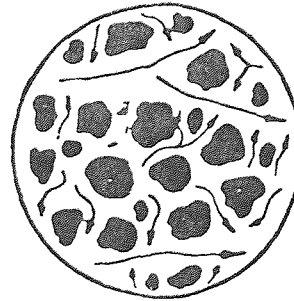
In the pilot demonstration of pneumatic fracturing carried out at AT&T Richmond Works fracture orientation was horizontal with a detectable maximum radius



BEFORE FRACTURE
(Diffusion Controlled)

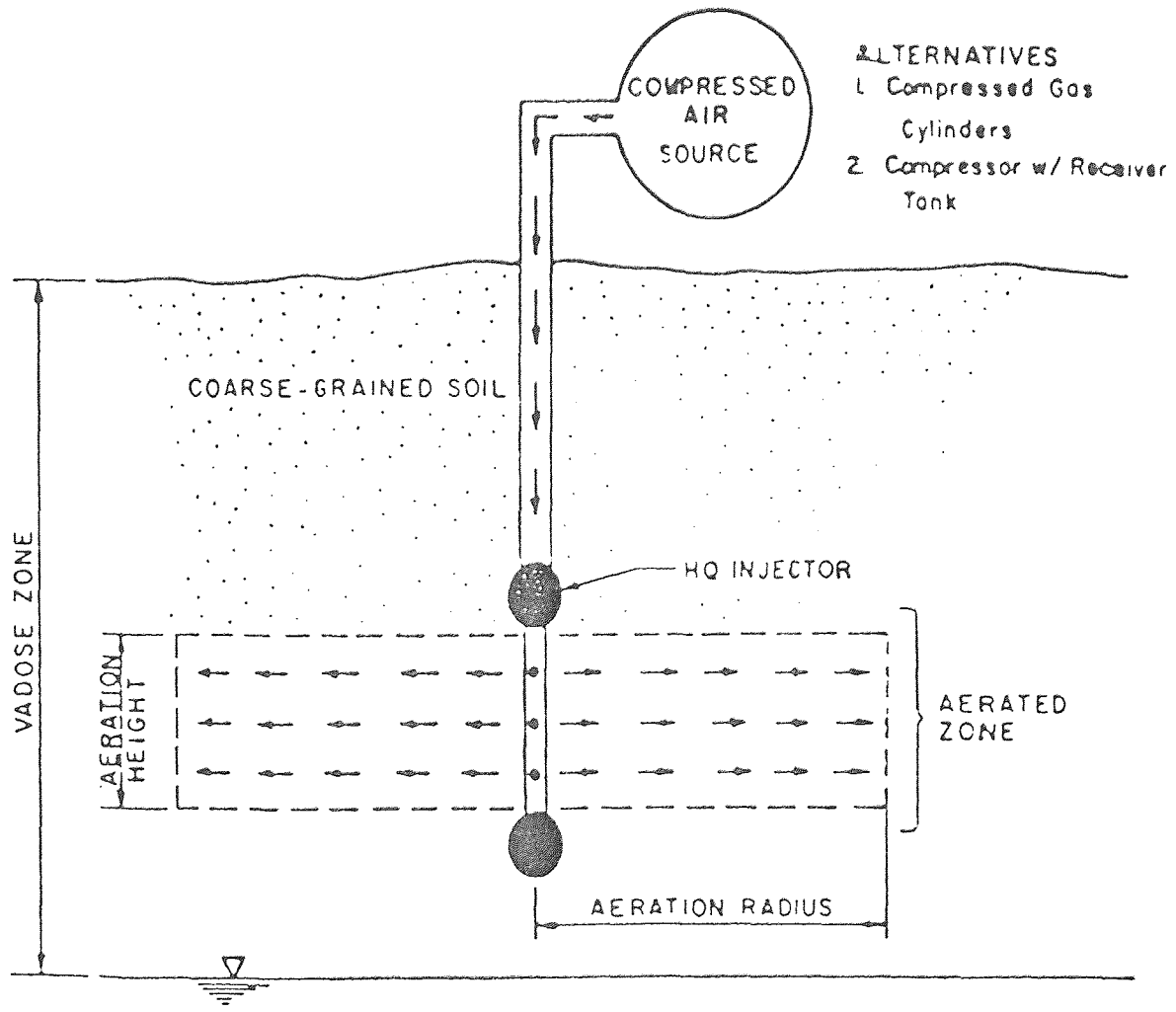


AFTER FRACTURE
(Convection & Diffusion Controlled)



DETAIL "A"
VAPOR MOVEMENT IN SOIL MICROSTRUCTURE

Figure 1 Pneumatic Fracturing Concept, Fine-Grained Soils



EXAMPLE

GIVEN. FLOW RATE = 900 C.F.M. FOR 2 MINUTES
POROSITY = 0.4
MOISTURE CONTENT = 5%
DRY UNIT WEIGHT = 100 LB./FT.³

RESULT AERATION RADIUS = 18.9 FT.
AERATION HEIGHT = 5 FT.

Figure 2 Pneumatic Aeration Concept, Coarse-Grained Soils

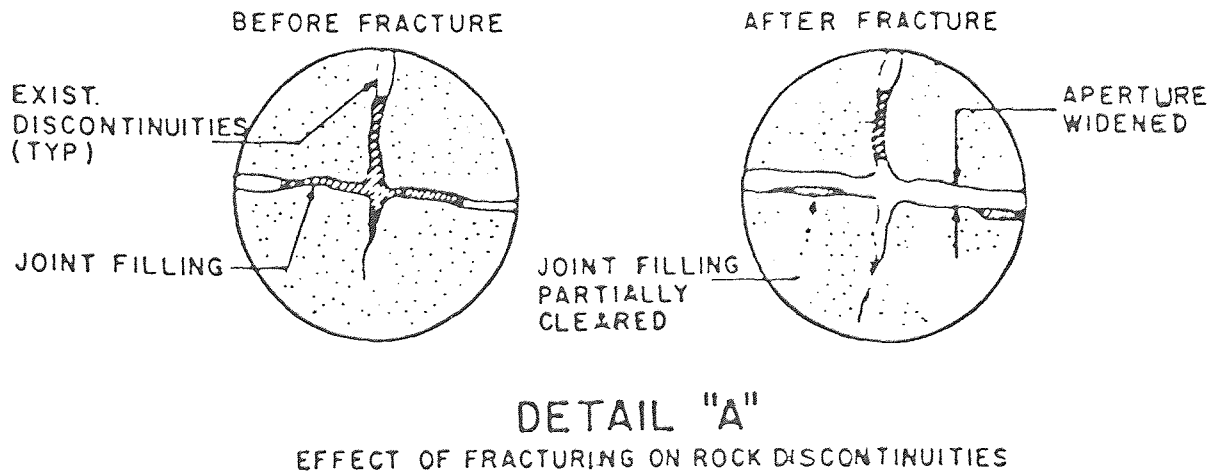
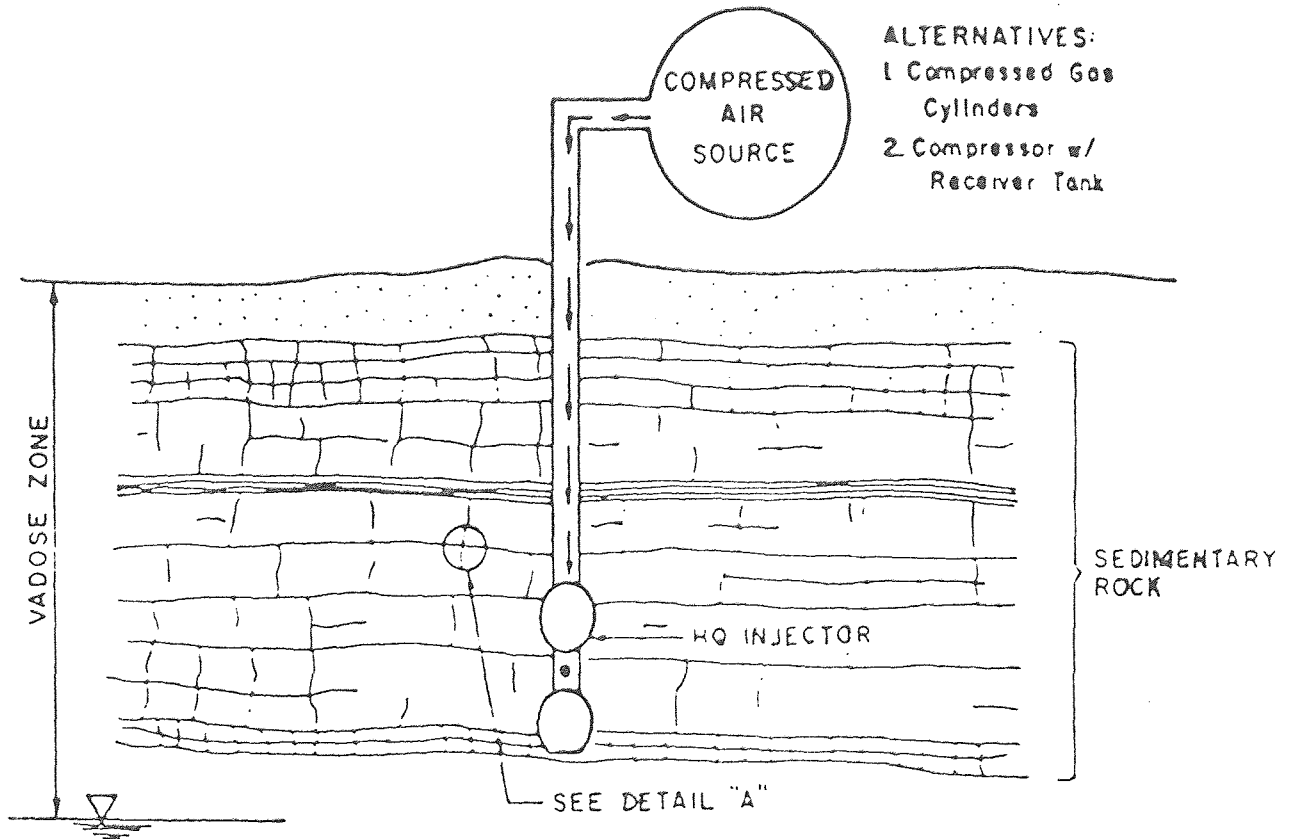


Figure 3 Pneumatic Fracturing Concept, Rock Formations

of twelve feet. The shape of the fracture was approximately elliptical, and the preferred propagation direction was northward. Refer to Figures 1.4 and 1.5 for the well schematic and pneumatic fracturing injector/packers, respectively (Schuring 1992). The cracks were typically 3 feet apart and the average crack width was 0.13 in.

1.2.2 Catalytic Oxidation

Hydrocarbons contaminated with halogen compounds are emitted from many industrial processes. These compounds are often found in trace amounts and are best disposed of by incineration. One such example involves chlorinated hydrocarbons used commercially as stripping and dry cleaning solvents, refrigerants, transformer fluids, etc. These materials can become toxic wastes for which cost effective and environmentally sound methods of disposal are being sought. Incineration provides an option which can be applied to a wide range of such wastes. Thermal incineration requires high temperatures, with concurrent high fuel costs and the potential for formation of acid gases such as NO_x . Frequently, more highly chlorinated, and hence, more toxic products than the starting materials are formed. Use of a catalytic approach results in lower temperatures, less toxic products, and greater flexibility when compared to homogeneous thermal processes.

1.2.2.1 Catalytic Destruction of Trichloroethylene

A noble metal catalyst was evaluated for its ability to oxidize two chlorinated compounds, viz., methylene chloride (CH_2Cl_2) and trichloroethylene (TCE, C_2HCl_3). It was shown that the catalyst containing 1.5% Pt on γ -alumina/monolith with 400 channels/in² can effectively oxidize 150 ppm TCE in air at 450° C and space velocities of 30,000 v/v/hr. Activity was monitored for 100 hours at these conditions and found to decrease linearly with time to about half of its fresh activity. On the assumption that

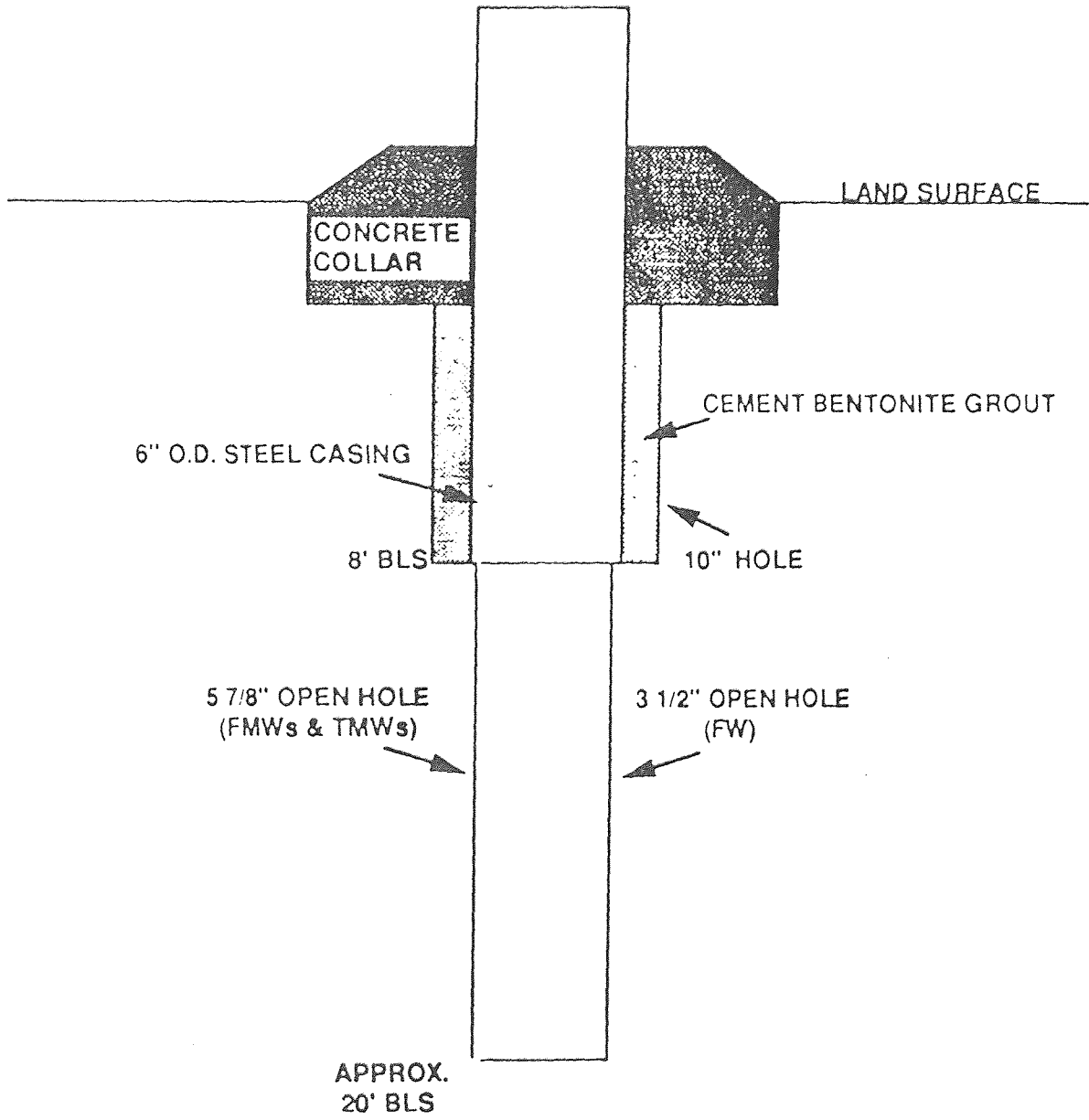


Figure 4 Well Schematic

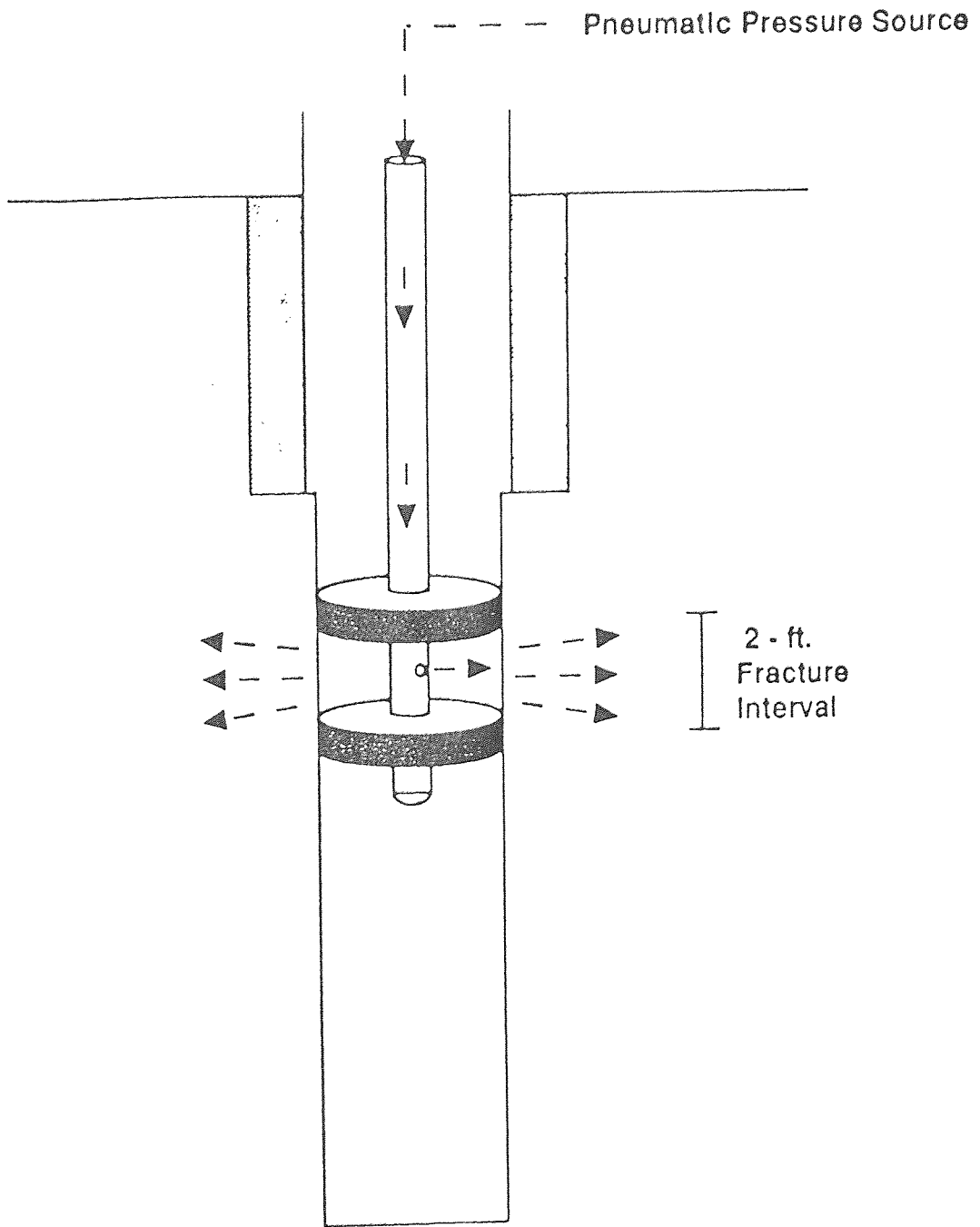


Figure 5 Pneumatic Fracturing Injector/Packers

halocarbon oxidation obeys a first order rate law, kinetics show that the oxidation of TCE occurs with an activation energy of 18 kcal/mol. Experiments with varying amounts of oxygen show no effect on the rate law, thus allowing good representation as a first order destruction of the chlorocarbons (Shaw et al., 1991).

Catalytic destruction of contaminants depends on both surface kinetics and mass diffusion rates. Accurate analysis of the chemical and physical details requires a comprehensive model that allows the simultaneous occurrence of both factors. A primary target of the experimental work is the determination of surface kinetic parameters, particularly activation energy (E) and pre-exponential factor (A).

1.2.3 HCL Removal and Heat Injection

In the model presented here, the hot flue gas from the incinerator or catalytic oxidizer needs to be cleaned-up to reduce air-pollution. All commercial incinerator effluent and gas control systems use alkaline scrubbers to remove HCl, SO_x, P₂O₅, etc. However, this approach invariably transforms an air-pollution problem into a water pollution problem. The captured acid gases are then confined in a much smaller volume than they would have occupied in the atmosphere, albeit larger mass. Therefore, a process to adsorb or react these gases with solid materials that are stable at elevated temperatures is being proposed. It has been shown that calcium compounds adsorb HCl quantitatively up to 1000 K. Over 80% of the calcium content of the sorbent CaCO₃ was utilized. This approach is anticipated to reduce the cost of air pollution control, conserve energy and reduce overall capital investment (Shaw et al., 1993).

As part of the HSMRC SITE project, it has been demonstrated that calcium carbonate (CaCO₃) can be used in a practical system to remove 1,000 to 5,000 ppm HCl, with about 80% Ca utilization in very small particles of CaCO₃ (less than 400 mesh) at 500° C from a N₂ stream, but at a high pressure drop. In order to reduce pressure drop and increase available surface for reaction, 6-20 mesh CaCO₃ was

calcined at 700° C and reacted with 2,000 ppm HCl in N₂ at 500° C resulting in over 20% calcium utilization compared with less than 10% calcium utilization with uncalcined material. Very rough estimates indicate that a once-through CaCO₃ system designed for continuous removal of 14 lb HCl/hr would roughly have a 20% advantage over heat exchange and conventional HCl scrubbing (Shaw et al., 1993).

A system consisting of two calcium carbonate (CaCO₃) adsorber beds has been conservatively designed to remove all hydrogen chloride (HCl) from the combustion of 1,000 ppm(v) trichloroethylene (TCE) in a catalytic oxidizer. It was assumed that the first year operation in the clean-up of a contaminated site would be conducted over some 8,000 hours and the concentration of TCE would vary from 1,000 ppm(v) to 100 ppm(v). The total amount of HCl produced in the first year will be 30 tons and assuming 50% calcium utilization efficiency, 83 tons of CaCO₃ would be needed. 50% calcium utilization efficiency has been achieved in the laboratory with calcined CaCO₃ powder (Shaw et al., 1993)

1.3 Objective

The main objective of this thesis was to develop better understanding of how heat is distributed in pneumatically fractured soil and how volatile organic compounds are removed from the fractures. In order to accomplish this, it was decided to mathematically model a non-steady state heat distribution system. The potential hydrocarbon pick-up would be integrated with the heat transfer model and includes increases in vapor pressure with temperature and diffusion into the flue-gas stream.

CHAPTER 2

HOT GAS INJECTION MODEL DESCRIPTION

2.1 Consolidated Model Description

2.1.1 Process Description

The HGI site remediation process is designed to increase the rate of in situ contaminant removal as part of a site remediation process system. It is anticipated that HGI will be used in conjunction with technologies that will augment flow and thermal destruction of contaminants. HGI involves different stages of contaminant removal with the main objective of decreasing the time and cost required to cleanup a contaminated site. The injection of hot gas into wells to enhance subsurface contaminant removal is a major component in a system that will help achieve this objective. The overall site demonstration program involves the use of pneumatic fracturing to open existing subsurface cracks or passages. This is followed by the application of vacuum extraction through a compressor/vacuum pump to remove air containing contaminant vapor. The contaminant is subsequently destroyed by passing the gaseous mixture through a catalytic oxidation unit producing water, carbon-dioxide and in the case of chlorocarbon contaminant, hydrogen chloride. The HCl may be removed by a second process involving dry scrubbing at elevated temperatures. Figure 2.1 presents a flow sheet of the site remediation process. Generally, hot gas for the injection phase is available as a result of this remediation process, but could be generated independently, if necessary.

The basic principle lies in the exponential dependence of vapor pressure on the inverse of temperature. Due to heating by HGI, there is an increase in the contaminant temperature and hence an exponential increase in vapor pressure leading to increased mass removal rates. It should be noted that the contaminant will redeposit in the

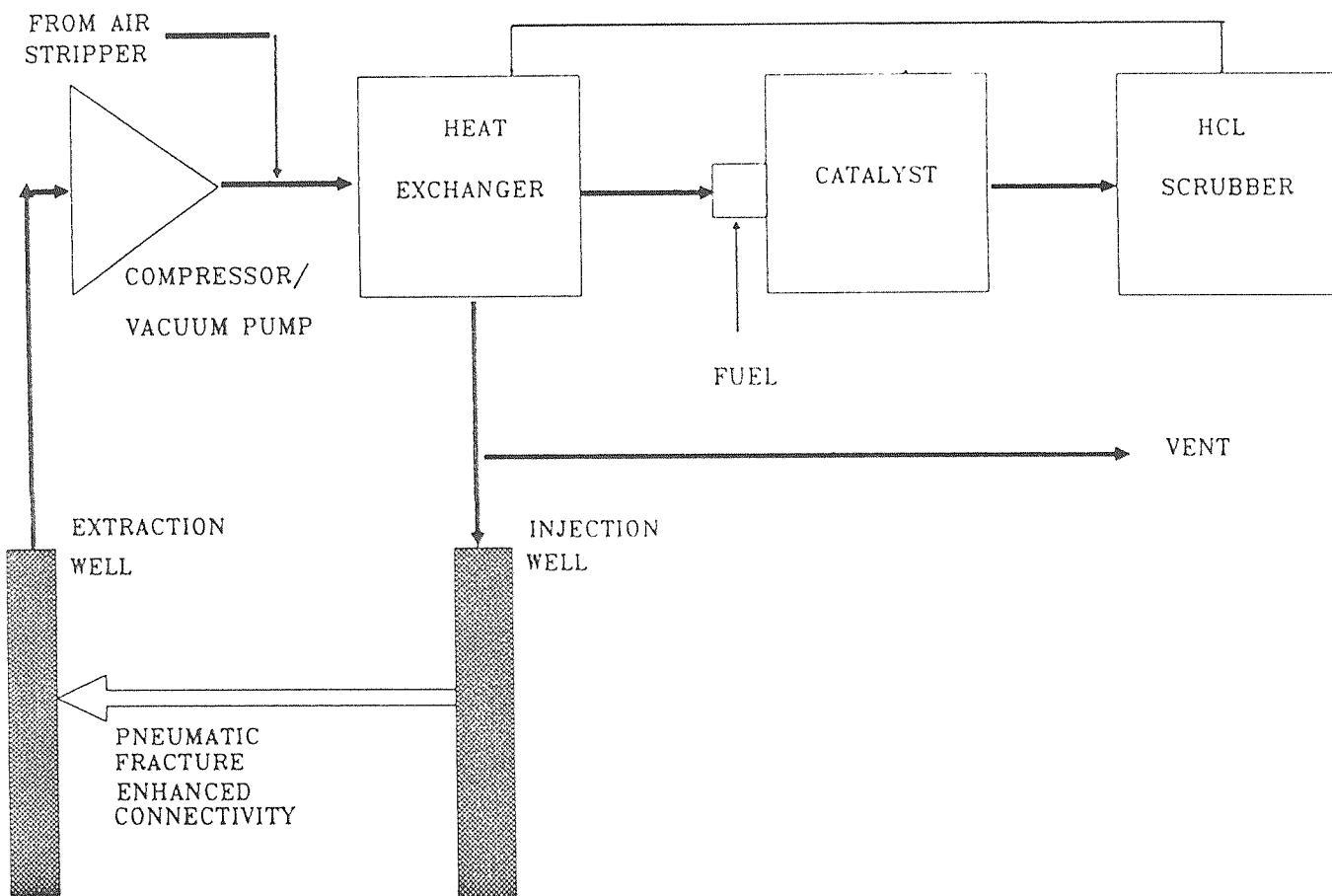


Figure 6 Pneumatic Fracture - Hot Gas Injection, Site Remediation Process Streams

subsurface cracks that have not been heated as the hot gas cools on its way to the extraction well. The system is most effective after a steady state is established which depends on the distance between the injection and extraction well.

2.1.2 Mathematical Model Description

A non-steady state ground heating model is necessary due to the poor conductivity and good heat capacity of the shale formation. Using the heat injection well as the radial center for a cylindrical coordinate system, a non-steady state numerical heat transfer model is used to determine ground temperature in three dimensions assuming uniform gas flow in the radial direction along horizontal fracture planes (due to the pneumatic fracturing effect). Flexibility in continued use of the model is accommodated by providing for user selection of the various input conditions relevant to the computation. The non-steady state temperature distribution thus obtained is used to estimate the mass removal rates by linking a heat transfer model to a mass transport model that has been developed.

Once the input parameters' conditions of interest are identified, the required node spacing for computational accuracy is determined along with the maximum time increments that can be used consistent with numerical stability requirements. Achievable subsurface non-steady state temperatures and gas phase temperatures over injection time periods extending to 8 days are determined as a function of radial position from the well and axial position from the fracture into the rock material. For each of these subsurface and gas phase temperatures at different nodes along the radial direction the mass removal rate is calculated as a function of crack surface temperature and time by assuming an initial average concentration on the pneumatically fractured surfaces.

The technical rationale will help design well spacing as well as estimate the benefits that can be realized in terms of contaminant mass removal rates and associated

costs. Hot gas is injected into the subsurface fissures which increases the contaminant temperature and the surrounding rock temperature. This characteristic temperature increase should be significant (i.e., doubling of TCE vapor pressure) and can be set by the user. Liquid vapor pressure is approximately an exponential function of the saturation temperature. For most liquids, this translates into a doubling of the vapor pressure for approximately every 10 degree Celsius temperature rise. The program uses this temperature difference to calculate the radial spread of heating from the well and the total volume of rock which achieves this increase. For nonporous rock, contaminant material would be expected to deposit along the fracture surfaces, and thus, the radial spread would be more important than the total volume. Once the model has been calibrated for a site, then selection of well spacing for the hot gas injection phase of a demonstration program can be based on model results. The translation of a significant temperature rise to double the vapor pressure results in increased contaminant diffusion rates thereby increasing contaminant mass removal rates.

2.2 Modeling Rationale

2.2.1 Heat Transfer Considerations

Analysis of HGI requires the use of a transient ground heating model due to the poor conductivity and good heat capacity of the subsurface rock formations. Using the heat injection well as the radial center for a cylindrical coordinate system, a non-steady state numerical heat transfer equation is used to determine ground temperature in three dimensions assuming uniform gas flow in the radial direction along horizontal fracture planes. This first model does not account for the presence of an extraction well and the resulting effect of extraction on the subsurface flow pattern. This extension is being provided by including the mass transport considerations to this model.

The equations summarized in section 2.3 have been developed on the basis of a *forward-difference* technique in that the temperature of a node at a future time increment is expressed in terms of the surrounding nodal temperatures at the beginning of the time increment.

For the non-steady state heat transfer problem represented here, the nodal network has been set-up assuming:

- Radial Symmetry from the axis of the injection well.
- Uniform spacing of fissures.
- Uniform diameter of cracks.
- Equally spaced nodes in the 'R'(radial) and 'Z'(axial) directions.

Figure 2.2 illustrates the type of nodal elements under consideration for each of the equations and are represented by the hatched region for node (i,j). The four basic equations for heat transfer are for nodes (0,0), (0,j), (i,0), (i,j). The combined conduction and convection equations are only for nodes (0,0) and (i,0). Nodes (0,j) and (i,j) represent only conduction.

Since the boundary conditions may change, depending on the type of contaminant distribution at each node, the task of choosing an appropriate time increment becomes an important criterion. To ensure stability, the time increment must be kept equal to or less than a value obtained from the most restrictive nodal equation. These stability equations are the equations defined in the next section. A detailed derivation has been included in Appendix-B. For modeling heat transfer the salient considerations are:

- Fracture flow is predominantly laminar and developed.
- Coefficient of heat transfer is constant.
- Heat transfer is highly time and space dependent due to the small diffusivity (10^{-6} m²/s) of the subsurface material.

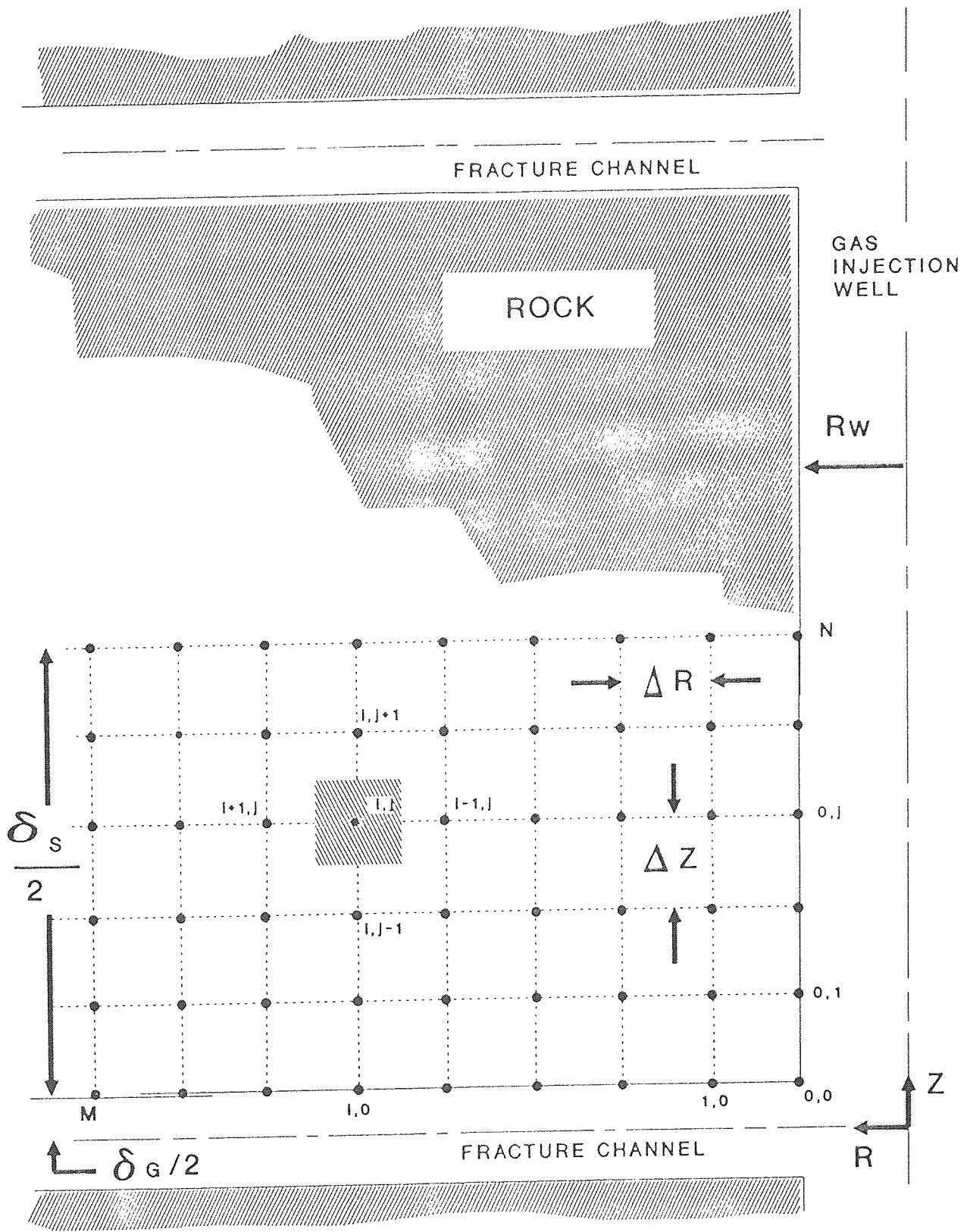


Figure 7 Subsurface Heating By Hot Gas Injection, Nodal Network

2.2.2 Mass Transport Considerations

An unambiguous description of the TCE mass removal rate (or TCE concentration in the extraction flow) requires knowledge of the subsurface distribution of the liquid contaminant. Since this is unknown, a variety of possible conditions need to be considered. Two limiting extremes correspond to no contamination (trivial case of zero TCE removal) and to uniform surface contamination over the entire subsurface flow region. During cold flow or the initial period of HGI, the extracted gas will be in temperature equilibrium with the subsurface rock. Consequently, given sufficient gas residence time or no mass transport limitation, the equilibrium vapor pressure of TCE would be established in the extracted gas. Assuming a subsurface temperature of 65° F this vapor pressure would be 0.0702 atm. which corresponds to a maximum concentration of 70,200 ppm at a total pressure of 1 atm.

As with most flow dominated processes, mass transport will be influenced by the Reynolds number. In the majority of the SITE tests, the measured gas flow was considerably less than 30 scfm. Using this value as a conservative estimate along with an average channel pressure of 1.5 atm and conservative evaluation of other properties at standard temperature of 60° F, the equation for Reynolds number becomes,

$$Re = 1512/R \quad (\text{where } R \text{ is the radial location in ft.})$$

Consequently, within a short distance from the injection well (less than 20 cm) the flow will be in the laminar regime. For developed, internal, laminar flow, the analysis and experimental results for both heat and mass transport indicate that the Nusselt (Nu) and Sherwood (Sh) Numbers are constant. For the conditions of the SITE tests, both the heat and mass transport coefficients (h and g_i) can be taken as constant along the channel length.

Two sub-processes to this process of mass removal that have been discussed here are:

- 1 Equilibrium vapor pressure at the gas-liquid interface.
- 2 Mass transport from the surface to the gas phase.

The process involving evaporating the contaminant is dependent upon the difference between the gas phase mass fraction of contaminant and the equilibrium mass fraction of contaminant at the boundary layer, which gives the driving force. A check on the mass transport is performed so that the amount removed can never exceed the amount present initially.

The removal rate can be estimated once the driving force is determined. This requires that the mass be balanced at any point in any cell. At every radial step a balance can be drawn on the mass of contaminant present, amount entering, amount transported and amount leaving. To estimate these, knowledge of the mass fraction of contaminant in gas from the previous cell is necessary. Initially this is 0 and as time progresses the hot gas starts picking up contaminant. The balance is drawn on every cell as follows:

$$M_{in}(i) = 60 \cdot \rho_a \cdot q_a \cdot dt \cdot MFG(i-1) \quad (1)$$

$$M_{out}(i) = 60 \cdot \rho_a \cdot q_a \cdot dt \cdot MFG(i) \quad (2)$$

$$M_p(i) = \rho_a \cdot V_i \cdot MFG(i) \quad (3)$$

Where, $M_{in}(i)$ = Mass of contaminant entering the i th cell, lbs

$M_{out}(i)$ = Mass of contaminant leaving the i th cell, lbs

$M_p(i)$ = Mass of contaminant in i th cell at the beginning of time step, lbs

$MFG(i)$ = Mass fraction of contaminant in gas in the i th cell

V_i = Volume of the i th cell based on crack width, ft^3

q_a = Flow rate of hot gas in CFM at solid temperature of cell i

ρ_a = Density of hot gas, lb_m/ft^3 at solid temperature of cell i
 dt = Time step, hrs.

The quantities representing the amount entering, leaving and that present depend solely on the mass fraction of contaminant in gas while, the amount transported from the surface depends on the difference between the equilibrium mass fraction and the gas phase mass fraction. To estimate the equilibrium mass fraction, the following relationships were used:

$$X_i = P_i/P$$

$$\text{MFE}(i) = \frac{X_i}{X_i + (1-X_i)M_a/M_b} \quad (4)$$

Where, X_i = mole fraction of contaminant (TCE)

P_i = equilibrium partial pressure (vapor pressure) of contaminant based on solid temperature along the radial nodes of the fracture channel, psia
 (refer Appendix-C for vapor pressure curve for TCE)

P = total pressure, psia

M_a = molar mass of air, 29 lbs

M_b = molar mass of contaminant, 131.39 lbs

To obtain the mass transported, the following equation was derived (refer to Appendix-B for derivation):

$$\dot{m}_i = \rho_a \cdot V_i \cdot \text{fac} \cdot (\text{MFE}(i) - \text{MFG}(i)) \quad (5)$$

Where, \dot{m}_i = mass transported in one time step, lbs

$$\text{fac} = (1 - e^{-rdt})$$

where, $r = 2g_i a_i / \rho_a V_i$;

g_i = mass transfer coefficient, $10.5 \text{ lb}_m / \text{ft}^2 \text{ hr}$

a_i = area of the i th cell

Therefore, the balance on any cell 'i' which gives the new mass of contaminant in the i th cell would be:

$$m_i = M_{in}(i) + M_p(i) - M_{out}(i) + \dot{m}_i \quad (6)$$

and the new mass fraction of contaminant in the gas would be:

$$MFG(i) = m_i / \rho_a V_i \quad (7)$$

Further, initial contaminant distribution on the surface was assumed to be $0.1 \text{ lb}_m / \text{ft}^2$ at every cell. If the mass of contaminant left on the surface be represented by $MLS(i)$, then initially,

$$MLS(i) = 0.1 a_i$$

This value needs to be updated based on the mass transported. Comparing the current value of $MLS(i)$ with the mass transported (\dot{m}_i) gives the correct value of actual mass transported. If the mass left on the surface at a particular cell is less than the mass transport (\dot{m}_i) at that cell, then it means that the mass transported needs to be updated to the value of mass left on the surface, because mass transport can reach a maximum value of only what is left on the surface at a particular cell. If the value of $MLS(i)$ is not reached, then $MLS(i)$ needs to be updated due to depletion of contaminant from the boundary layer.

Therefore,

$$MLS(i) = MLS(i) - \dot{m}_i \quad (8)$$

These calculations are repeated for the next time step and the total contaminant pickup can be assessed by summing the pickups at exit for every time step.

The mass transfer coefficient (g_i) in equation (5) is a function of Lewis number (Le) which in turn is a function of the Schmidt number (Sc) and the Prandtl number (Pr). The Schmidt number depends on the diffusion coefficient (D_{ab}) which gives the diffusivity of TCE in air. The mass transfer coefficient is given by:

$$g_i = \frac{h (Le)^{2/3}}{c_p} \quad (9)$$

Where, h = heat transfer coefficient, $5 \text{ Btu/hr.ft}^2. \text{ } ^\circ\text{F}$

Le = Lewis number

c_p = heat capacity of hot gas, $\text{Btu/lb}_m. \text{ } ^\circ\text{F}$

and the diffusion coefficient is given by:

$$D_{ab} = \frac{1.8583 \times 10^{-7} \sqrt{T^3}}{(\sigma_{ab})^2 \Omega_d} (1/M_a + 1/M_b) \text{ ft}^2/\text{hr} \quad (10)$$

Where, M_a = molar mass of air, lbs

M_b = molar mass of TCE, lbs

σ_{ab} = collision diameter, Å

Ω_d = collision integral for diffusion

2.2.3 Technical Rationale

For Hot Gas Injection, the surface temperature (and thus the contaminant temperature) will increase as heat is transferred from the gas to the surface. In this case, surface temperature will vary with radial distance from the HGI injection well. Since TCE concentration or mass fraction at the surface depends on the TCE vapor pressure and since the vapor pressure is an exponential function of temperature, the incremental addition of TCE mass flux due to each surface element will vary rapidly as a function of distance along the flow direction. The total amount of TCE removed at the extraction well will be an integration of the individual mass flux from each surface element. The surface elements near the injection well would contribute the majority of the mass flux (assuming that this region is not depleted of contaminant).

Detailed computation of contaminant (TCE) mass removal rates due to HGI requires combining a mass transport analysis, such as that given above, with a comprehensive heat transport analysis. The potential improvement in mass removal due to HGI can, however, be illustrated by recognizing the strong exponential variation of liquid (TCE or other contaminant) vapor pressure on temperature. For TCE, the vapor pressure, P_i (atm), as a function of temperature, t ($^{\circ}\text{C}$), is given as,

$$\ln P = A - \frac{B}{t+C}$$

$$P_i = P/760$$

Where, P = vapor pressure, mm Hg.

P_i = vapor pressure, atm

t = temperature, $^{\circ}\text{C}$

Effectively, for every 20°F , the vapor pressure would double, thereby greatly increasing the potential driving force for mass transport.

2.3 Equations

1. R-NODE 0, Z-NODE 0

Differential Equation

$$\frac{1}{r} \frac{\partial}{\partial r} \left(r k \frac{\partial T}{\partial r} \right) + \frac{\partial}{\partial z} \left(k \frac{\partial T}{\partial z} \right) + h \Delta T = \rho c_p \frac{\partial T}{\partial t}$$

Nodal Equation

$$\begin{aligned} q_s + k\pi \left(r_w + \frac{\Delta r}{2} \right) \frac{\Delta z}{2} \left(\frac{T_{1.0} - T_{0.0}}{\Delta r} \right) + k\pi \Delta r \left(r_w + \frac{\Delta r}{4} \right) \left(\frac{T_{0.1} - T_{0.0}}{\Delta z} \right) \\ = \rho c_p \pi \Delta r \left(r_w + \frac{\Delta r}{4} \right) \frac{\Delta z}{2} \left(\frac{T_{0.0}^\tau - T_{0.0}}{\Delta t} \right) \end{aligned}$$

Stability Equation

$$\Delta t < \frac{\rho c_p}{\frac{2h}{\Delta z} + \frac{k}{\Delta r} \frac{\left(r_w + \frac{\Delta r}{2} \right)}{\left(r_w + \frac{\Delta r}{4} \right)} + \frac{2k}{\Delta z}}$$

2. R-NODE 0, Z-NODE j ; $j > 0$

Differential Equation

$$\frac{1}{r} \frac{\partial}{\partial r} \left(r k \frac{\partial T}{\partial r} \right) + \frac{\partial}{\partial z} \left(k \frac{\partial T}{\partial z} \right) = \rho c_p \frac{\partial T}{\partial t}$$

Nodal Equation

$$k\pi\Delta r \left(r_w + \frac{\Delta r}{4} \right) \left(\frac{T_{0,j-1} - T_{0,j}}{\Delta z} \right) + k\pi\Delta r \left(r_w + \frac{\Delta r}{4} \right) \left(\frac{T_{0,j+1} - T_{0,j}}{\Delta z} \right) \\ + k\pi \left(r_w + \frac{\Delta r}{2} \right) \Delta z \left(\frac{T_{i,j} - T_{0,j}}{\Delta r} \right) = \rho c_p \pi \Delta r \left(r_w + \frac{\Delta r}{4} \right) \Delta z \left(\frac{T_{0,j}^{\tau} - T_{0,j}}{\Delta t} \right)$$

Stability Equation

$$\Delta t < \frac{\rho c_p}{\frac{2k}{\Delta z^2} + \frac{k}{\Delta r^2} \left(\frac{r_w + \frac{\Delta r}{2}}{r_w + \frac{\Delta r}{4}} \right)}$$

3. R-NODE i, Z-NODE 0

Differential Equation

$$\frac{1}{r} \frac{\partial}{\partial r} \left(r k \frac{\partial T}{\partial r} \right) + \frac{\partial}{\partial z} \left(k \frac{\partial T}{\partial z} \right) + h \Delta T = \rho c_p \frac{\partial T}{\partial t}$$

Nodal Equation

$$\begin{aligned} & k\pi \left(r_w + i\Delta r + \frac{\Delta r}{2} \right) \frac{\Delta z}{2} \left(\frac{T_{i+1,0} - T_{i,0}}{\Delta r} \right) + k\pi \left(r_w + i\Delta r - \frac{\Delta r}{2} \right) \frac{\Delta z}{2} \left(\frac{T_{i-1,0} - T_{i,0}}{\Delta r} \right) \\ & + 2k\pi\Delta r (r_w + i\Delta r) \left(\frac{T_{i,1} - T_{i,0}}{\Delta z} \right) + 2h\pi\Delta r (r_w + i\Delta r) (T_{g_i} - T_{i,0}) \\ & = \rho c_p 2\pi\Delta r (r_w + i\Delta r) \frac{\Delta z}{2} \left(\frac{T_{i,0}^\tau - T_{i,0}}{\Delta t} \right) \end{aligned}$$

Stability Equation

$$\Delta t < \frac{\rho c_p}{\frac{2h}{\Delta z} + \frac{k}{\Delta r^2} + \frac{2k}{\Delta z^2}}$$

4. R-NODE i, Z-NODE j

Differential Equation

$$\frac{1}{r} \frac{\partial}{\partial r} \left(r k \frac{\partial T}{\partial r} \right) + \frac{\partial}{\partial z} \left(k \frac{\partial T}{\partial z} \right) = \rho c_p \frac{\partial T}{\partial t}$$

Nodal Equation

$$2k\pi\Delta r (r_w + i\Delta r) \left(\frac{T_{i,j-1} + T_{i,j+1} - 2T_{i,j}}{\Delta z} \right)$$

$$+ k\pi \left(r_w + i\Delta r + \frac{\Delta r}{2} \right) \Delta z \left(\frac{T_{i+1,j} - T_{i,j}}{\Delta r} \right)$$

$$+ k\pi \left(r_w + i\Delta r - \frac{\Delta r}{2} \right) \Delta z \left(\frac{T_{i-1,j} - T_{i,j}}{\Delta r} \right) = \rho c_p 2\pi\Delta r (r_w + i\Delta r) \Delta z \left(\frac{T_{i,j}^\tau - T_{i,j}}{\Delta t} \right)$$

Stability Equation

$$\Delta t < \frac{\rho c_p}{\frac{2k}{\Delta z^2} + \frac{k}{\Delta r^2}}$$

2.4 Integration of Heat and Mass Transport

A combined heat and mass transport model is necessary for prediction of contaminant mass removal rates. The heat transfer model developed initially was modified to account for the heat of vaporization. Since two sub-processes were involved in the case of mass transport, both these sub-processes were linked to the heat transfer model. The temperature of the rock at the crack surface is used to determine the equilibrium vapor pressure in the concentration boundary layer. The rock temperature is, of course, coupled to the gas temperature rise in the heat transfer model. Finally, the difference between the contaminant concentration in equilibrium (expressed as a mass fraction) and the concentration in the gas stream gives the driving force used in computing the mass transport. The integration lies basically in generating data for the rock surface temperature distribution based on gas temperature rise, and using this data for predicting contaminant removal rates. It is assumed that contaminant distribution is initially uniform throughout the channel length.

CHAPTER 3

TEST CASES

3.1 Heat Transfer Iterations

The initial model consisting only of the heat transfer equations was used to predict the temperature distribution at the nodes along the fracture channel and the temperature rise in rock surface. Also, the model was used to predict the spread in feet and the volume of rock achieving this temperature rise. The program, after accepting the user input values, gives the output temperature distribution, spread of this temperature and the volume of rock achieving this temperature rise. The program was exercised for various iterations. Characteristic curves were determined for 100 SCFM at 700° F. The results of this trial run are summarized in Figure 3.1.

The nodal network has been limited to a maximum grid size of 100x100 for the heat transfer model. Crack separations are assumed to be 3 ft apart and the crack width is 0.130 in. Time increments used in all these calculations are 10^{-4} min. With the above mentioned parameters as default values, the temperature of the gas was set to 700° F with a time array starting from 1 hour up to 24 hours. For a typical 24 hr test period, the gas flow was uniform at 100 scfm and the extraction rates were kept slightly higher than the injection rates. As anticipated, Figure 3.1 shows the temperature rise curve was more steep for 3 connecting fractures when compared to one connecting fracture. This result is in agreement with field test data that had a fracture width of 0.008 in. Further the radial spread (ft) for every 20° F rise (characteristic temperature increase) was obtained. This value is the distance inside the rock surface that has achieved a 20°F temperature rise after any time period. Similarly, the volume of rock (ft³) achieving this characteristic temperature increase was also obtained.

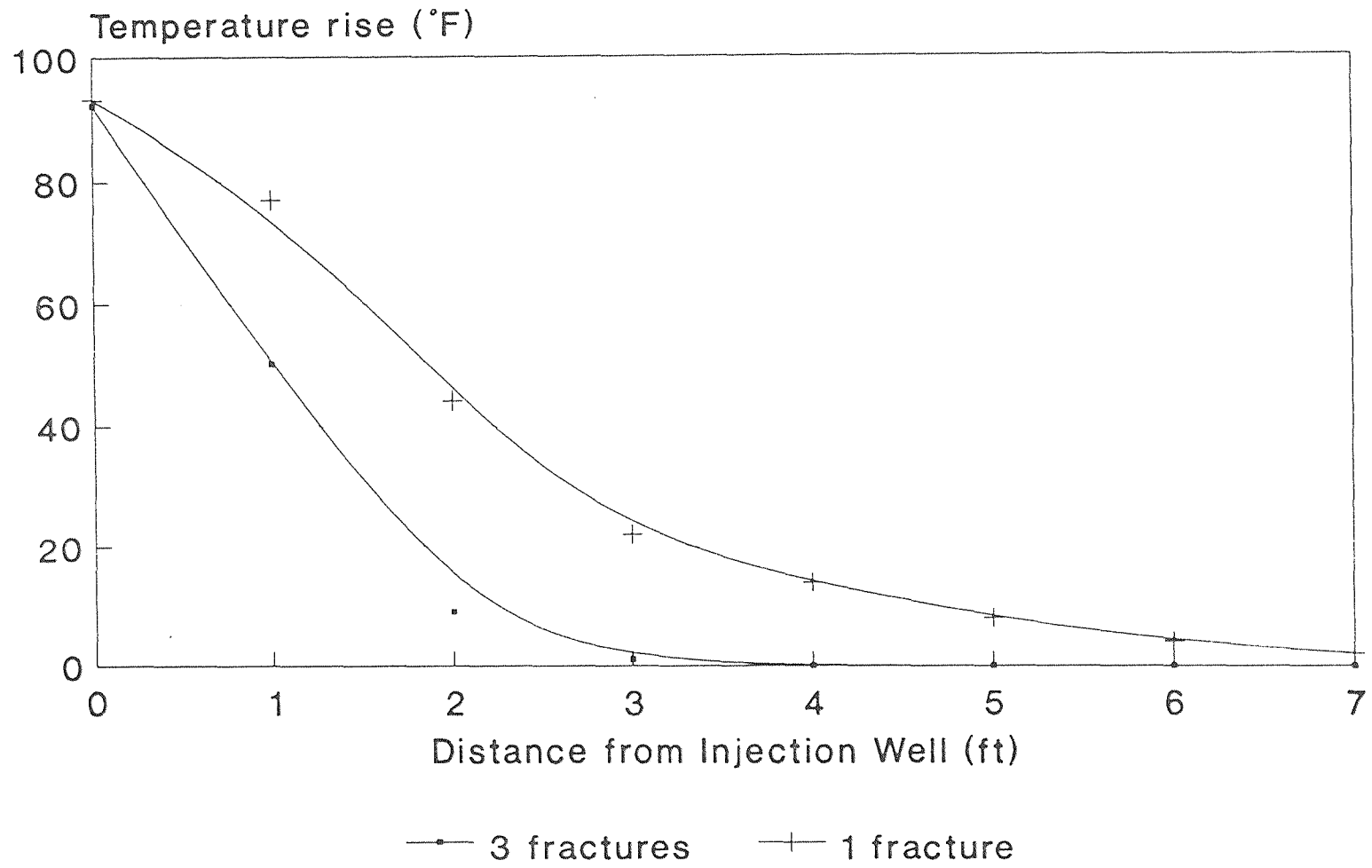


Figure 8 Subsurface Heating By HGI - 24 Hr. Test

3.2 Mass Transport Iterations

From the temperature distributions obtained from the initial model, the mass removal rates were estimated corresponding to the temperatures along the nodes in the radial direction of the fracture channel where the contaminant distribution is assumed. Mass removal rates are obtained as described in Chapter 2 from a single model which utilizes the difference in surface equilibrium and gas-phase concentrations as the driving force for flow. Contaminant distribution was assumed to be uniformly spread over the channel length with an initial concentration of 0.1 lb/ft^2 . Such a distribution could be extended to liquid pools at particular nodes. This was carried out over a 24 hr period and the results are summarized in this chapter. As anticipated, removal rates approximately double for every 20° F temperature rise.

Since the mass removal rates depends on the temperatures at the nodes, and the mass fraction of contaminant in the gas, these values play a major role in obtaining accurate results. Solid temperature distribution was obtained from the heat transfer model, which was used in calculating the vapor pressure of the contaminant and hence the equilibrium mass fraction of contaminant at the boundary layer. As already mentioned in Chapter 2, the difference between the mass fraction of contaminant, in equilibrium and gas phase provides the driving force for mass transport. In some instances, the calculated value for mass transferred during a time step could exceed the value of mass left on the surface. A check is made to assure that the value of the mass transported does not exceed the value of mass left on the surface. These calculations are performed iteratively for time steps of 10^{-4} minutes with data being printed to a file at every 1 hour time interval. The mass transport iterations work mainly by updating two quantities, the mass fraction of contaminant in gas (MFG) and the mass of contaminant left at the surface (MLS).

The value of the mass fraction of contaminant in gas is updated to obtain the new concentration of contaminant in gas phase as the hot gas moves to the next node. The amount of contaminant picked up by the gas will control the amount that can be picked up from subsequent nodes. Also the amount of contaminant that can be picked up can never exceed the amount present at that node. To account for this the value of *MLS* is updated which gives the amount of TCE left at the surface and is the maximum amount that can be picked up by the gas.

CHAPTER 4

DISCUSSION OF RESULTS

4.1 Heat Transfer and Temperature Distribution

The results obtained from trial runs are basically analyzed and presented in a convenient form. As already stated in Chapter 3, all discussions, interpretations and conclusions have been based on one standard run of 100 SCFM flue gas at 700° F. For the heat model, the fracture temperature distributions are plotted at radial well intervals as shown in Figure 4.1. Plots for different hours of gas flow are given. It can be seen from the graph that the temperature distribution at the fracture increases with the hours of gas flow, because as time progressively increases with the gas injection remaining constant at 700° F, the temperature at the nodes also tend to achieve a steady state with time. It should be noted that the highest temperature is found near the injection well during any time period. All these findings are in line with anticipated results.

Similarly, fracture temperature distributions in terms of the hours of flow have been indicated in Figure 4.2. This plot clearly shows the temperature drop along the fracture channel from inlet to exit along the radial direction and also the relative temperature difference (increase) with time at a particular radial distance from the inlet well. This plot is merely a rearrangement of the previous data but gives a very clear picture.

Having indicated the fracture channel distribution temperature rise in the interior nodes can also be represented. Figure 4.3. indicates the rock temperature, after 24 hours of gas flow at 100 SCFM and 700° F, as a relative position of radial distance and the distance from the crack (Z-direction) and basically represents the distribution for any node (i,j). Similar results have been obtained for 4 hours and 8 hours of injection.

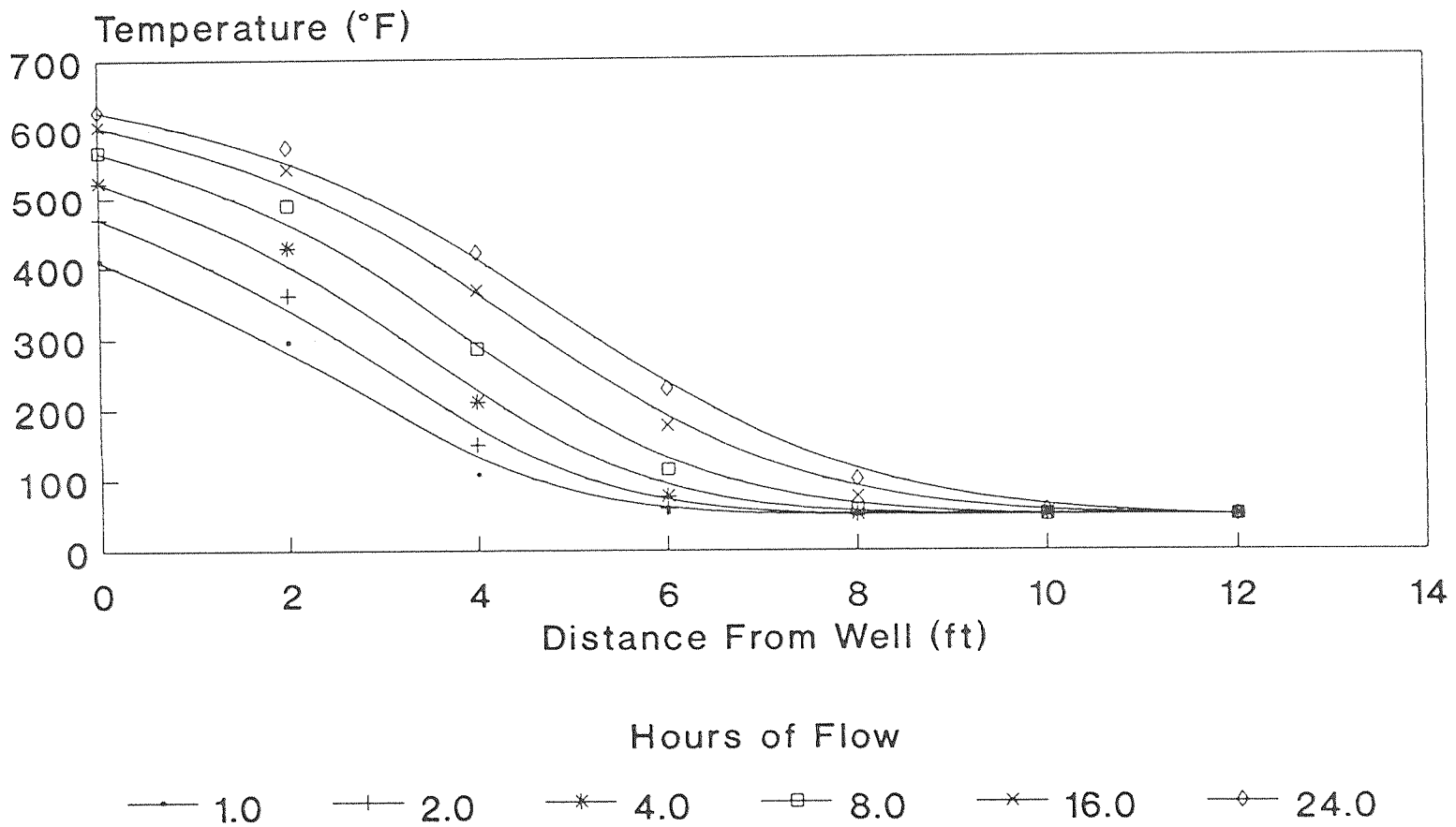


Figure 9 Fracture Temperature - 100 SCFM Flue Gas at 700 °F
Temperature Vs Distance from Well

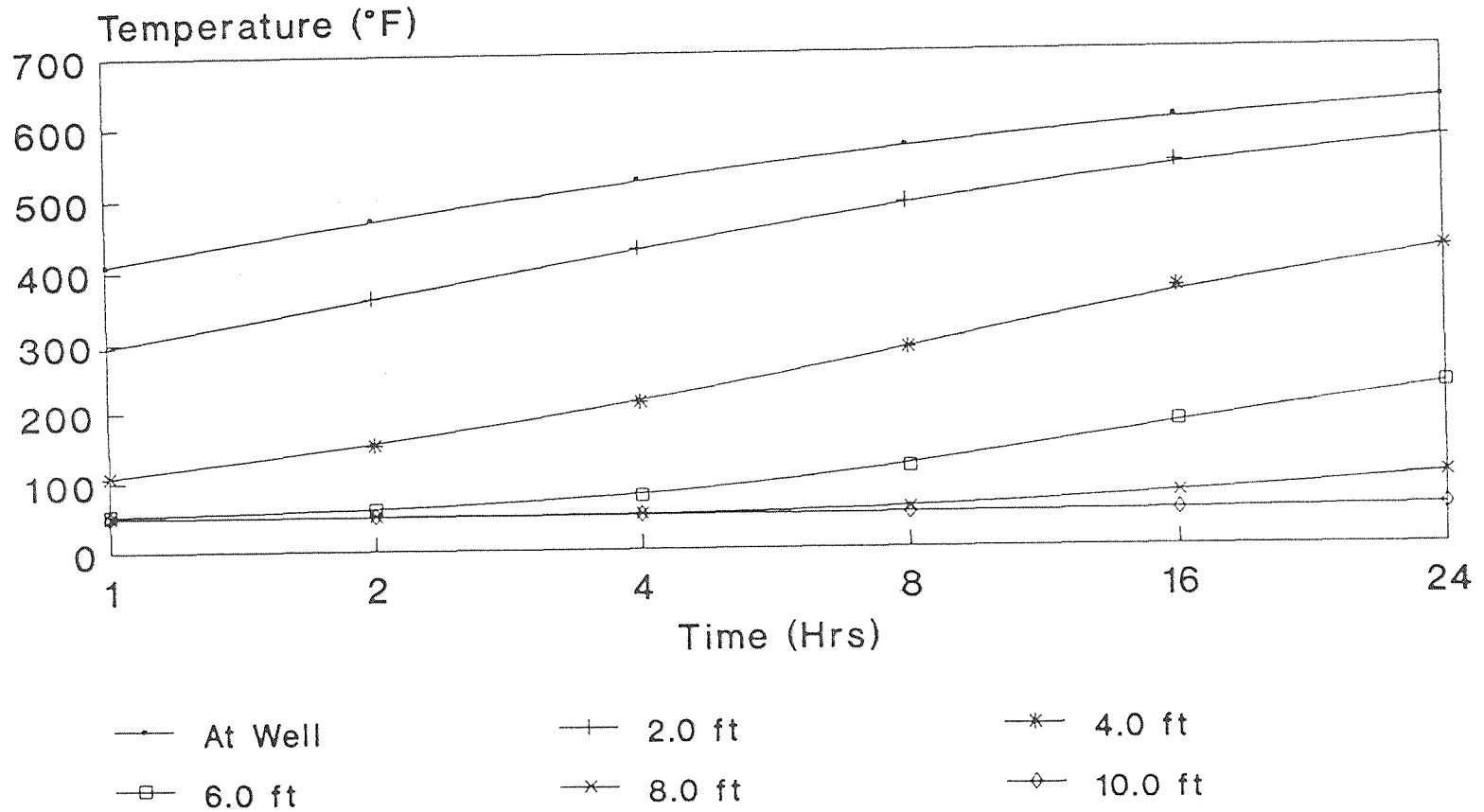


Figure 10 Fracture Temperature - 100 SCFM Flue Gas at 700 °F
Temperature Vs Time

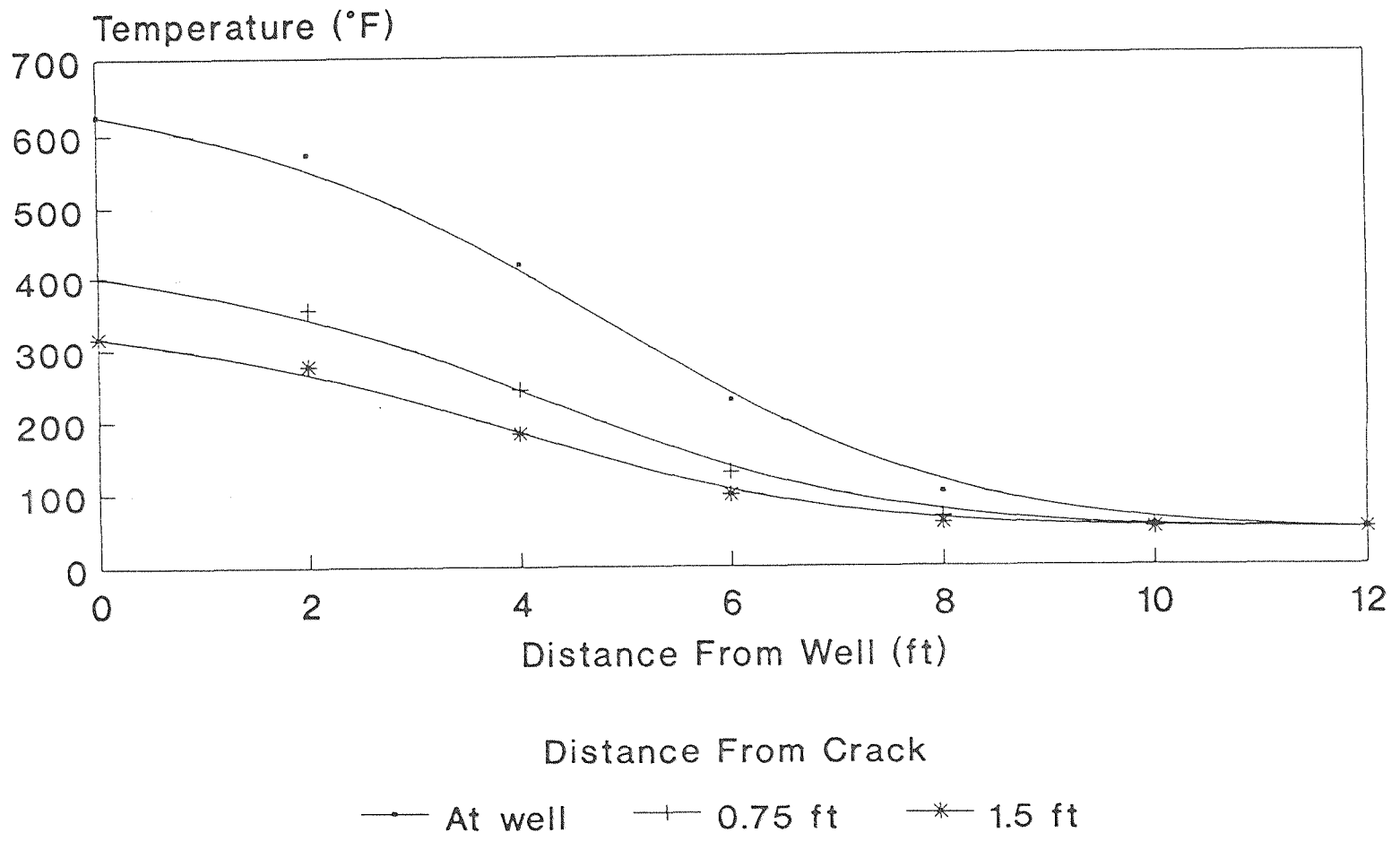


Figure 11 Rock Temperature - 100 SCFM Flue Gas at 700 °F
24 Hr. Injection

4.2 Mass Transport and Mass Residual Distribution

From the discussion in the previous section, it follows naturally that having obtained the temperature distributions for flue gas injected at 700° F and 100 scfm, the mass removal rates of the contaminant can be estimated. Both mass fraction of contaminant in the gas and mass of liquid remaining on the surface are obtained from the calculations. The contaminant pickup by the hot gas is given by the mass fraction of contaminant in gas and by the amount of TCE left at surface in the boundary layer. So, a plot of these two variables has been made which summarizes the results. The results are for a typical 24 hour flow period and the plots have been made for exactly the same time steps used in the heat transfer model.

The results have been plotted for the residual TCE at every node at the boundary layer, against time as shown in Figure 4.4 and also for the contaminant pick-up at every node in the gas phase, against time as shown in Figure 4.5. Both these plots have been carried out over all the nodes from entry to exit for different hours of flow of hot gas. It can be seen from Figure 4.4 that the amount of TCE left at any point of time is the least near the well which in turn means that the contaminant pick-up is highest at the well. Initially the gas starts picking up contaminant at a fast rate, because the hot gas is not laden with contaminant, leaving very little at the surface, in a very short time. But progressively the temperature of the rock and gas drop and the gas cannot pick up any more contaminant because there is no driving force. Further downstream, the driving force reverses and the gas laden with contaminant deposits the contaminant back on the surface. This can be inferred by referring to Figure 4.4. The concentration of contaminant at every hour of flow reaches the initial value near the exit (45th node). Figure 4.5 explains this mechanism clearly too, as the pick-up is high near the well because gas temperatures are highest at the entry.

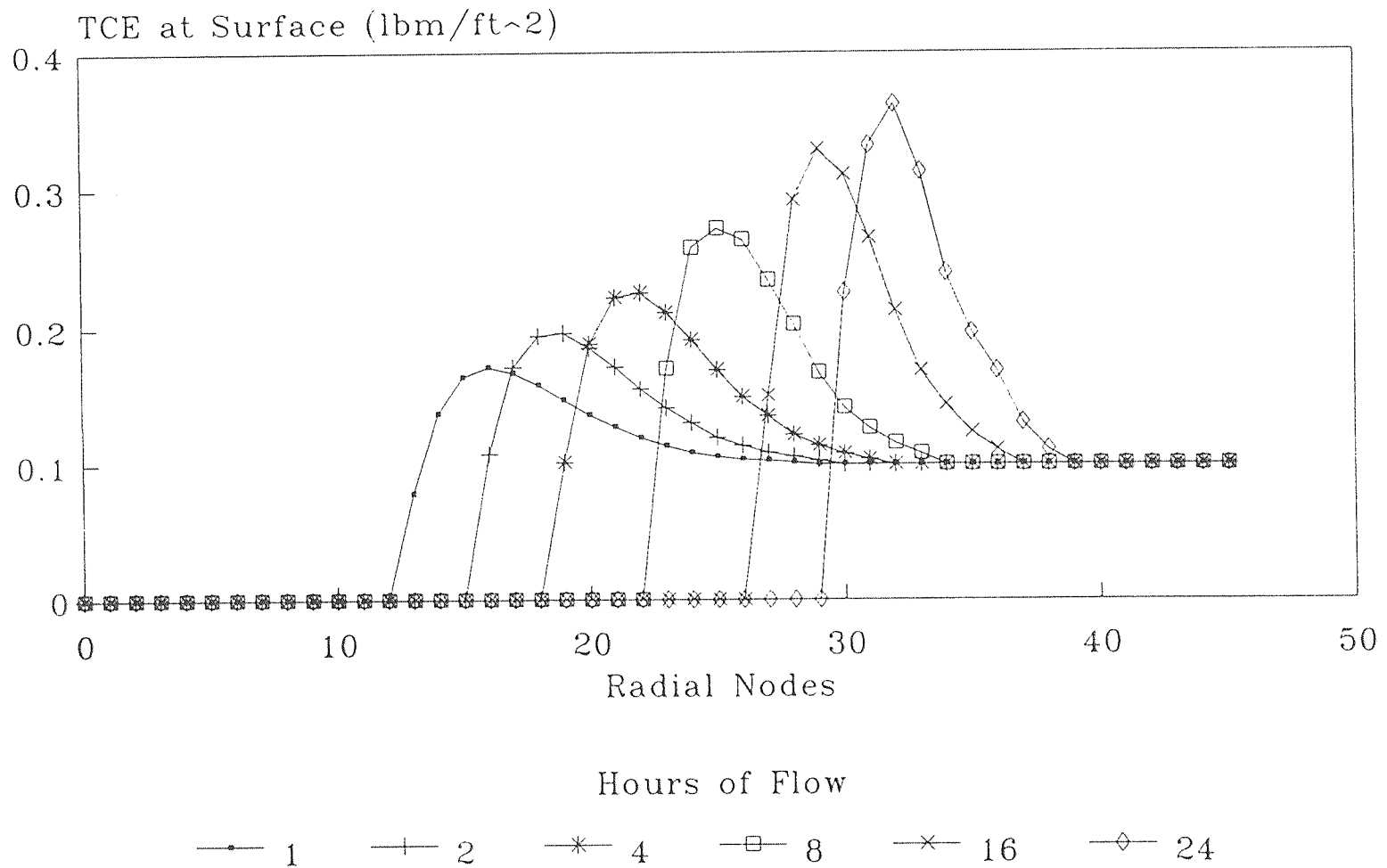


Figure 12 TCE at Surface at Different Times and Nodes

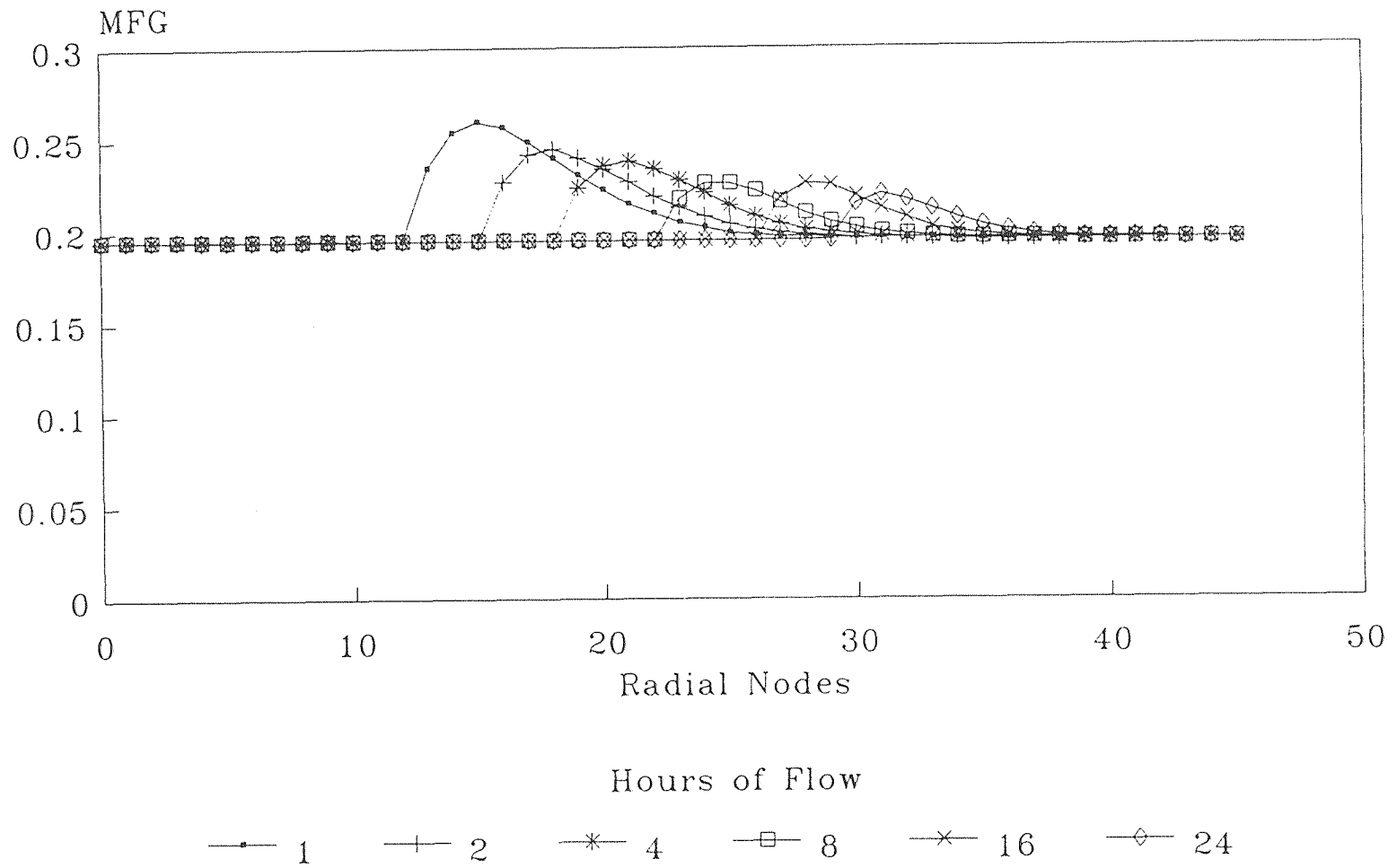


Figure 13 Mass Fraction of Contaminant in Gas for Different Times and Nodes

CHAPTER 5

MODEL VERIFICATION

The model developed here is an integration of heat and mass transport. The model is actually a computer program (developed in FORTRAN) which utilizes various input parameters to predict temperatures and contaminant removal rates from the subsurface. In order to check the suitability of such a model for an engineering application, it must be tested. This chapter discusses the outcome of the tests conducted to check the internal consistency of the model developed. Since the model developed here deals both with the heat and mass transfer, its accuracy can be checked by carrying out a heat and mass balance.

For the model developed here, an energy balance was calculated and the results obtained were exact sparing a few round-off errors. The energy balance was carried out along the channel length and involved evaluating three quantities. The amount of heat entering a node, the amount of heat used for heating the rock and vaporizing the liquid contaminant, and the amount of heat leaving the node. This would involve the conduction and convection heat flow in and the conduction heat flow out. This has been done at every node over a 24 hour period. The results are included in Appendix-D and the energy balance calculations appear below the removal rate calculations at each node.

For the mass balance check of the model, the output from the program gives the amount of TCE left in the channel and the amount of TCE removed from the existing concentration at each time increment. These values represent the amount of TCE in pounds over the entire fracture area. For the mass balance, the sum of the total pick up of contaminant over the flow period and the mass left at the surface at every time step, must equal the initial mass present.

Therefore, if

$X =$ total contaminant pick up in lbs over 24 hrs,

$Y = \Sigma$ Mass left at surface, lbs

and $Z =$ initial mass present $= 0.1 * \Sigma A(x)$, lbs

then, $Z = X + Y$

This was verified and found to be almost exact with an error of 0.5%. This error could be attributed to minute round-off errors which occur as a result of formatting the output from the program.

Verification of the model has been included as part of the consolidated output which includes total analysis time, fracture temperature at the extraction well, the number of radial and axial nodes, solid temperature distributions, gas temperatures at each node, and the mass removal rates. Appendix-D gives the output in the above mentioned order. The results have been obtained for a 24 hr analysis and the output shows the values in the following order:

- 1 Total runtime is 1440 minutes (24 hours).
- 2 Fracture temperature at extraction well is 50° F.
- 3 The number of radial nodes is 45 and the number of axial nodes is 10.
- 4 Temperature distribution in the solid rock starts at 612° F and ends at 50° F for one set of 45 radial nodes in the axial direction. This procedure has been repeated for all the 10 axial nodes.
- 5 Mass residual rates and mass removal rates at every radial node corresponding to gas temperatures starting from 698° F to 50° F.

CHAPTER 6

SUMMARY AND CONCLUSIONS

The model developed here is capable of achieving its objective in the sense that the predicted contaminant removal rates is close to the anticipated removal rates. From the exponential dependence of vapor pressure on temperature, mass transported is expected to double for approximately every 20 °F temperature rise. Comparison with existing preliminary data shows that the removal rates predicted by the model are roughly the same as those observed from actual field tests. However, with the model developed, significant removal rates may be noticed only with time which may not be the actual case.

Addition of the mass transport equations to the heat transfer model has made the model a more reasonable representation. Although suitable data do not exist to validate the model, it seems likely from the initial results obtained that the current model is a good starting point for further research.

The effect of heat of vaporization has been incorporated to refine the heat balance equations. Although this may not alter the results to a large extent, it is a correct modification of the model.

For the mass transport model, two sub-processes both of which are interdependent have been discussed. The value of the gas phase mass fraction is updated by performing a mass balance at every cell using equation(6) in Chapter 2. Similarly, the equilibrium concentration at the boundary layer is estimated using the vapor pressure of the contaminant. The driving force for transport is the difference between the equilibrium mass fraction and the gas phase mass fraction. The amount of contaminant removed by the HGI process can be calculated from its mass fraction in the gas exiting the radial node furthest from the well.

The model accuracy was verified by incorporating the heat and mass balance equations. Further field tests have been planned after which a specific direction can be obtained as to the corrections needed in the model. One of the major tasks would be to break down the existing model into modules for easy analysis and modification. Such modulization would facilitate future improvements, such as modifications of existing features, inclusion of new capabilities, enhanced input/output, or the use of a different coordinate system.

CHAPTER 7

RECOMMENDATIONS

The existing model is based on the assumption that the Hot Gas Injection into the fracture channels is radially spread along the fracture length. Extension of this could be made to include flow pattern modification between injection and extraction wells as shown in Figure 7.1.

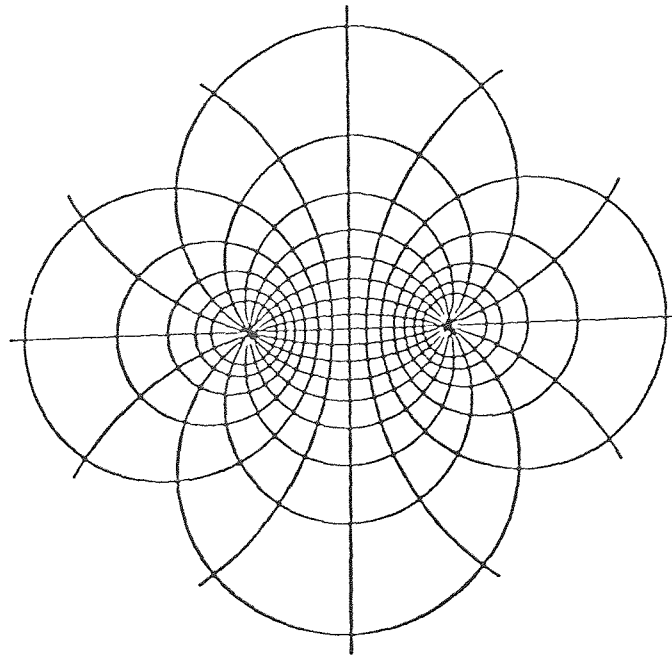


Figure 14 Flow Pattern Modification

Infinite replenishment of contaminant at the fracture channel from the rock material has been dealt with here. Modification needs to be made to incorporate finite replenishment rates to account for bleed from porous rock.

One of the major improvements that could be done in this research area is to study the dynamics of fluid flow for mass removal through the fracture channels. The

topic of fluid dynamics has not been covered in this work. Fluid dynamics and gas dynamics considerations should enhance the capabilities of the model several fold.

One other area of particular interest may be the heat transfer through the injection well wall. The injection well wall has been considered as insulated and the heat transfer from the gas to the surrounding rock material while injection has not been considered and hence not modeled. This could be done as an addition to the model.

APPENDIX-A

PROGRAM CODE

```
PROGRAM HOTROCKF
PARAMETER (PI=3.1416,MMAX=101,NMAX=101,INDEX=3,IOUTMAX=20,
&IVARMAX=16)
*   ! MMAX=maximum number of radial nodes
*   ! NMAX=maximum number of axial nodes
*   ! INDEX=number of effective vol and radial spread parameters
*   ! IOUTMAX=maximum number of time points for saved data
*   ! IVARMAX=number of parametric variables
* REAL VARIABLES
*   ! DR,DZ: incremental radial & axial distances (ft)
*   ! PA,QA,TA: air pressure (kPa), flow (cfm) & temp (F)
*   ! CPA,RHOA: air heat capacity (Btu/lbm/F) & density (lbm/ft^3)
*   ! CPS,RHOS: solid heat capacity (Btu/lbm/F) & density (lbm/ft^3)
*   ! KS,TS: solid conductivity (Btu/hr/ft/F) & init temp (F)
*   ! HS,HC: fracture separation (ft) & crack height (in)
*   ! DTIME,DT: time difference used in computation (hrs)
*   ! TDIFF: temp increase (F) to achieve good result
*   ! TEFF: temperature (F) associated with tdiff
*   ! RUNTIME: total injection time (hours)
*   ! TF: final gas temperature (F)
*   ! Q,A1,A2,A3: temporary variables
* REAL ARRAY VARIABLES
*   ! T(0:MMAX,0:NMAX): solid temp (F)
*   ! TT(0:MMAX,0:NMAX): new solid temp (F)
*   ! VOL(INDEX,IOUTMAX): volume (ft^3)
*   ! REFF(INDEX,IOUTMAX): radial spread (ft)
*   ! TG(0:MMAX): gas phase temp (F)
*   ! A(0:MMAX): convective heat trans area (ft^2)
*   ! H(0:MMAX): convection coeff (Btu/hr/ft^2/F)
*   ! TIME(0:IOUTMAX): data output times (min)
*   ! PARM(0:IVARMAX): assigns parametric variables to real array
*   ! RLOOP(i,j): Major loop information i=1,2,3 loop A,B,C
*   ! (j=1) lower limit, (j=2) step size, (j=3) no. of var. pts.
* INTEGER VARIABLES
*   ! IA,IB,IC: dummy variables
*   ! IRUN: run number to be assigned by user
*   ! COUNT,CMAX: data output counter, maximum number for count
```

```

*   ! NLIM,MLIN: scaling loop limit for display purposes
*   ! W,X,Y,Z: loop counters
*   ! M,MM,N,NN: radial, radial+1, axial, axial+1 =node numbers
*   ! I,II: long integers for use as needed
*   ! LOOP(i): Major Loop Information
*   (0) counts loops activated- maximum number=3
*   (n) gives the parm index number for loop n
* CHARACTER VARIABLES
*   ! FOUT,FIN: assigned to output to file or input to file
*   ! CH: key reading string
*   ! RUNS,COUNTS: string associated with run and count
*   ! FNUM,FN: code associated with data file
*   ! WTITLE: title for display
*   ! FPATH,PREFNAME: front part incl root and mid part of directory
*   ! FULLFNAME: complete file path name
* LOGICAL VARIABLES
*   ! PRTRESULTS: output results to printer
*   ! FILEDATA: output results to disk directory data
*   ! SPENT: gas temperature = initial rock temperature
*   ! STABLE: time step used < maximum allowable time step
*   ! DONE: exercise control on while computation loop
*   ! DATAOUT: time to output data to file or print
*
  INCLUDE 'SPINATTR.HDR'
  IMPLICIT REAL*4(A-H,O-Z)
  REAL M1(0:100), MI(0:100), MIN(0:100)
  REAL QIN(0:100), QROCK(0:100)
  REAL RW, QOUT(0:100), SUM
  REAL MOUT(0:100), MDOT(0:100)
  REAL MFE(0:100), MFG(0:100)
  REAL MNEW(0:100), MOL(0:100)
  REAL KS, HFG, VI(0:100)
  REAL APV, BPV, CPV, MA, MB
  REAL BV(0:100), G(0:100)
  REAL MLS(0:100), EFFMASS(0:100)
  REAL PV1(0:100), EQ1(0:100)
  REAL FAC(0:100), R
  REAL*8 DVAL,VAL
  INTEGER*2 COUNT,CMAX,X,Y,Z,IERR,ISERROR
  INTEGER*4 I,II,IMARK1(3),ILEN,LEFT$,MID$,ILF,IMID,IDCH1,W
  CHARACTER CH*1,COUNTS*2,CC2*2,CCC2*2,
&FULLFNAME*25,FPATH*13,PREFNAME*4,FNUM*2,FN*2,CLK*11,
&WTITLE*39,CLIST1(3)*37,GETCH*1,C1*1,C2*2,C3*3,C4*4,C5*5,ACHAR*5,
&D$*2,H$*2,M$*2,BIGCHAR*40,CLIST2(4)*15,C8*8,C11*11,DAT*8

```

```

LOGICAL
PRTRESULTS,FILEDATA,SPENT,STABLE,DONE,DATAOUT,LVAL,FEXIST,
&SUMMARY
DIMENSION
T(0:MMAX,0:NMAX),TT(0:MMAX,0:NMAX),VOL(INDEX,IOUTMAX),

&REFF(INDEX,IOUTMAX),TG(0:MMAX),A(0:MMAX),H(0:MMAX),RLOOP(0:
3),
&TIME(0:IOUTMAX),PARM(0:IVARMAX),ISPACE(0:5),LOOP(0:3)
*
* (PROGRAM START, SET STRINGS, NUMERICS, & CONTROLS)
CALL CLS
WTITLE='SUBSURFACE HEATING BY HOT GAS INJECTION'
IRUN=0
PRTRESULTS=.FALSE.
FILEDATA=.FALSE.
SUMMARY=.TRUE.
SPENT=.FALSE.
STABLE=.FALSE.
DONE=.FALSE.
DATAOUT=.FALSE.
PREFNAME='CASE' !(alternatives include SITE, COMP, ROCK)
*
* (USER DECISIONS ON DATA STORAGE OPTIONS)
CALL OPENWIND (0,0,0,24,79,3,1+8)
CALL TITLE (0,WTITLE,0,0,1+8)
CALL CLRB(0)
CALL OPENWIND (5,1,42,8,77,3+8,1+112)
CALL TITLE (5,'SELECTIONS MADE',0,0,1+112)
CALL CLRB(5)
W=0
CALL BLDB (5,W,0,'SHOW RESULTS TO SCREEN',1+112)
CALL DEFWIND (10,6,2,10,40,3,4+48)
CALL TITLE (10,'SELECTION PROCEDURE',0,0,4+48)
CALL CLRB(10)
CALL BLDB (10,0,0,' <SPACE BAR> to select/deselect ',4+48)
CALL BLDB (10,1,0,' <F7> to mark all <F8> to unmark all',4+48)
CALL BLDB (10,2,0,' <ENTER> to return final selections ',4+48)
CALL OPENWIND (1,1,2,5,40,3,1+48)
CALL TITLE (1,'DATA STORAGE OPTIONS',0,0,1+48)
CALL CLRB(1)
CLIST1(1)='PRINT ONLY SUMMARY RESULTS'
CLIST1(2)='PRINT ALL RESULTS TO PAPER'
CLIST1(3)='SEND RESULTS TO DATA FILE'
IMARK1(1)=1

```

```

IMARK1(2)=0
IMARK1(3)=0
CALL MARK (1,CLIST1,3,1,IMARK1)
IF (IMARK1(1).EQ.0) SUMMARY=.FALSE.
IF ((SUMMARY).AND.(IMARK1(2).EQ.0)) THEN
W=W+1
CALL BLDB (5,W,0,'SUMMARY PRINTING ONLY ',1+112)
END IF
IF (IMARK1(2).EQ.1) THEN
PRTRESULTS=.TRUE.
W=W+1
CALL BLDB (5,W,0,'RESULTS WILL BE PRINTED',1+112)
END IF
IF (IMARK1(3).EQ.1) THEN
FILEDATA=.TRUE.
W=W+1
CALL BLDB (5,W,0,'RESULTS WILL BE SAVED TO FILE',1+112)
END IF

```

*

* (IF DATA IS TO BE FILED DETERMINE CORRECT FILE CODE AND FILE NUMBER)

```

IF (FILEDATA) THEN
CALL DEFWIND (10,7,2,10,40,3,4+48)
CALL TITLE (10,'SELECTION PROCEDURE',0,0,4+48)
CALL CLR(10)
CALL BLDB (10,0,0,' < ARROW KEYS > to highlight selection ',4+48)
CALL BLDB (10,1,0,' < ENTER > to return selection ',4+48)
CALL OPENWIND (2,1,2,6,40,3,1+48)
CALL TITLE (2,'DATA FILE NAME OPTIONS',0,0,1+48)
CALL CLR(2)
CALL BLDB (2,0,0,' C:\ZDATA\HOT\ rr##.HOT',1+48)
CALL DEFCHOICE ('CASE',2,21,1)
CALL DEFCHOICE ('SITE',3,21,2)
CALL DEFCHOICE ('COMP',4,21,3)
CALL DEFCHOICE ('ROCK',5,21,4)
CALL DOMENU (ISEL,PREFNAME,1+48,0)
W=W+1
CALL BLDB (5,W,0,'FILENAME = '//PREFNAME//'rr##.HOT',1+112)

```

*

```

FPATH='C:\ZDATA\HOT\'
W=W+1
CALL BLDB (5,W,0,'FILEPATH = '//FPATH,1+112)
DO IRUN = 1, 99
WRITE(FNUM,'(I2.2)') IRUN
FULLFNAME=FPATH//PREFNAME//FNUM//'00.HOT'

```

```

LVAL=FEXIST(FULLFNAME)
IF (.NOT.LVAL) EXIT
END DO
IF (IRUN.GT.99) THEN
CALL CLS
CALL OPENWIND(10,8,18,15,61,3,4+112)
CALL TITLE(10,'PROGRAM TERMINATED',0,0,4+112)
CALL CLR(10)
CALL BLDB (10,1,1,'RUN NUMBER 99 EXCEEDED FOR FILENAME '//
&PREFNAME,4+112)
CALL BLDB (10,2,1,'PRESS ANY KEY TO EXIT TO DOS SCREEN
THEN',116)
CALL BLDB (10,3,1,'RESTART PROGRAM AND SELECT NEW
FILENAME',116)
CALL CUROFF
CALL TONE(440,50)
CALL ANYKEY
CALL CURON
CALL CLS
STOP
ELSE
DO X = IRUN+1, 99
WRITE(FN,'(I2.2)') X
LVAL=FEXIST(FPATH//PREFNAME//FN//'00.HOT')
IF (LVAL) EXIT
END DO
IF (X.LT.100) THEN
CALL OPENWIND(10,7,2,13,40,3,4+112)
CALL TITLE(10,'WARNING',0,0,4+8+128)
CALL CLR(10)
CALL BLDB(10,1,0,'STORED RUN NUMBERS NOT SEQUENTIAL
',4+112)
CALL BLDB(10,2,0,'PRESS <A> TO ABORT TO DOS AND
CORRECT',4+112)
CALL BLDB(10,3,0,'PRESS <C> TO OVERWRITE EXISTING DATA
',4+112)
CALL TONE(440,100)
DO WHILE (.NOT.DONE)
CH = GETCH(Z)
IF ((Z.NE.2).AND.((CH.NE.'C').OR.(CH.NE.'A')))) THEN
CALL BEEP
DONE=.FALSE.
ELSE IF (CH.EQ.'A') THEN
CALL CLS
STOP

```



```

ELSE IF (CH.EQ.'C') THEN
  DONE=.TRUE.
END IF
END DO
DONE=.FALSE.
END IF
END IF
W=W+1
  CALL BLDB (5,W,0,'NEXT ASSIGNED RUN NUMBER (rr)=
'//FNUM,1+112)
  ELSE
  IRUN=1
  WRITE(FNUM,'(I2.2)') IRUN
  PREFNAME='INFO'
  END IF
*
* (IDENTIFY THE TIMES AT WHICH DATA OUTPUT IS TO OCCUR)
  DO X = 1, 20
  TIME(X)=0
  END DO
  TIME(1)=60.0
  DO X = 2, 5
  TIME(X)=2.0*TIME(X-1)
  END DO
  TIME(6)=1440.0
  DO X = 7, 9
  TIME(X)=2.0*TIME(X-1)
  END DO
  CMAX=9
  CALL OPENWIND (4,1,2,23,40,3+8,1+48)
  CALL TITLE (4,'DATA SAVE/DISPLAY TIMES',0,0,1+48)
  DO WHILE (.NOT.DONE)
  CALL CLR(4)
  CALL LOCATEW (4,0,1)
  CALL PRINTW (4,'Time in minutes and (dd/hh/mm)')
  NLIM=0
  DO X = 1, CMAX
  CALL LOCATEW (4,X,1)
  WRITE(C2,'(I2.2)') X
  Z=INT(TIME(X))
  WRITE(C5,'(I5)') Z
  CALL PRINTW (4,'Time('//C2//')='//C5//' ')
  MLIM=MOD(Z,1440)
  WRITE(D$, '(I2.2)') (Z/1440)
  WRITE(H$, '(I2.2)') (MLIM/60)

```

```

WRITE(M$, '(I2.2)') MOD(MLIM,60)
CALL PRINTW (4, ' (//D$//''//H$//''//M$//')')
END DO
IF (CMAX.LT.15) THEN
CALL OPENWIND (1,17,41,23,78,0,1+8)
CALL CLR(1)
CALL OPENWIND (1,17,3,23,39,3,4+48)
ELSE
CALL OPENWIND (1,17,41,23,78,3,4+48)
END IF
CALL TITLE (1, 'PROCEDURE', 0, 0, 4+48)
CALL CLR(1)
CALL BLDB (1, 0, 0, 'MAX ARRAY 20 MAX TIME 99999 min', 4+48)
CALL BLDB (1, 1, 0, 'ENTER <D##> deletes array no. ##', 4+48)
CALL BLDB (1, 2, 0, 'ENTER <INTEGER> add new time (min)', 4+48)
CALL BLDB (1, 3, 0, 'ENTER <E> to end procedure', 4+48)
CALL BLDB (1, 4, 0, 'ENTER RESPONSE HERE =>', 4+48)
IF (CMAX.LT.15) THEN
CALL OPENWIND (2, 22, 26, 22, 30, 0, 4+112)
ELSE
CALL OPENWIND (2, 22, 64, 22, 68, 0, 4+112)
END IF
CALL CLR(2)
CALL LOCATEW (2, 0, 0)
CALL AREAD(ACHAR, ILEN)
CALL CTOS(ACHAR, IDCH1)
ILF=LEFT$(IDCH1, 1)
CALL STOC(ILF, C1)
IF (C1.EQ.'E') THEN
DONE=.TRUE.
CALL CLR(0)
ELSE IF (C1.EQ.'D') THEN
IMID=MID$(IDCH1, ILEN-1, 2)
CALL STOC(IMID, C2)
DVAL=VAL(C2)
IERR=ISERROR()
I=INT(DVAL)
IF ((IERR.NE.0).OR.(I.GT.CMAX)) THEN
CALL BEEP
ELSE
DO X= I, CMAX-1
TIME(X)=TIME(X+1)
END DO
TIME(CMAX)=0
CMAX=CMAX-1

```

```

END IF
ELSE IF ((C1.GE.'0').AND.(C1.LE.'9')) THEN
DVAL=VAL(ACHAR)
IERR=ISERROR()
I=INT(DVAL)
IF (IERR.NE.0) THEN
CALL BEEP
ELSE
DO X = 1, CMAX
IF (TIME(X).GT.I) EXIT
END DO
IF (I.NE.TIME(X-1)) THEN
DO Y = CMAX+1, X+1, -1
TIME(Y)=TIME(Y-1)
END DO
TIME(X)=I
CMAX=CMAX+1
END IF
END IF
ELSE
CALL BEEP
END IF
END DO ! (END of do while)
DONE=.FALSE.

```

*

* (SET DEFAULT PARAMETERS USED IN PROGRAM TEST)

```

PARAM(0)=IVARMAX
PARAM(1)=45.0
PARAM(2)=100.0
PARAM(3)=700.0
PARAM(4)=0.245
PARAM(5)=1.063
PARAM(6)=155.0
PARAM(7)=0.177
PARAM(8)=50.0
PARAM(9)=20.0
PARAM(10)=3.0
PARAM(11)=0.13
PARAM(12)=45
PARAM(13)=10
PARAM(14)=0.30
CALL CLS
CALL OPENWIND (1,0,0,18,58,3,1+8)
CALL TITLE (1,'SUBSURFACE AND HOT GAS PARAMETERS',0,0,1+8)
CALL CLR(1)

```

```

CALL OPENWIND (2,0,58,18,79,3,1+8)
CALL TITLE (2,'VARY TO : VALUES',0,0,1+8)
CALL CLR(2)
CALL OPENWIND (3,18,0,24,79,3,4)
CALL TITLE (3,'MODIFICATION PROCEDURE',0,0,4)
CALL CLR(3)
CALL LOCATEW (1,0,0)
PRINT*,' GAS STREAM PARAMETERS'
PRINT '(4X,A33,F8.3,A5)', ' 1-Pressure .....',
&PARM(1), ' psia'
PRINT '(4X,A33,F8.3,A4)', ' 2-Fracture flow rate .....',
&PARM(2), ' cfm'
PRINT '(4X,A33,F8.3,A2)', ' 3-Temperature .....',
&PARM(3), ' F'
PRINT '(4X,A33,F8.3,A10)', ' 4-Heat capacity .....',
&PARM(4), ' Btu/lbm/F'
PRINT*,' ROCK ZONE PARAMETERS'
PRINT '(4X,A33,F8.3,A12)', ' 5-Thermal conductivity .....',
&PARM(5), ' Btu/hr/ft/F'
PRINT '(4X,A33,F8.3,A9)', ' 6-Density .....',
&PARM(6), ' lbm/ft^3'
PRINT '(4X,A33,F8.3,A10)', ' 7-Heat capacity .....',
&PARM(7), ' Btu/lbm/F'
PRINT '(4X,A33,F8.3,A2)', ' 8-Initial temperature .....',
&PARM(8), ' F'
PRINT '(4X,A33,F8.3,A2)', ' 9-Target temperature increase ..',
&PARM(9), ' F'
PRINT '(3X,A34,F8.3,A3)', ' 10-Crack separation .....',
&PARM(10), ' ft'
PRINT '(3X,A34,F8.3,A3)', ' 11-Crack width .....',
&PARM(11), ' in'
PRINT '(3X,A34,I4)', ' 12-Radial nodes .....',
&INT(PARM(12))
PRINT '(3X,A34,I4)', ' 13-Axial nodes .....',
&INT(PARM(13))
PRINT '(3X,A34,F8.3,A3)', ' 14-Radial increment .....',
&PARM(14), ' ft'
CALL BLDB (3,0,0,'To change parameter ENTER'//
&' <(ITEM #) (NEW VALUE)>',4)
CALL BLDB (3,1,0,'To specify a range ENTER'//
&' <(ITEM #) (INITIAL VALUE) (FINAL VALUE) (INCREMENT)>',4)
CALL BLDB (3,2,0,'To exit procedure ENTER <E>',4)
CALL BLDB (3,3,0,'Use spaces to separate multiple entries'//
&' MAXIMUM of 3 variable loops',4)
DO X = 0, 3

```

```

LOOP(X)=0
RLOOP(X,3)=1
END DO
CALL BLDB (3,4,0,'ENTER RESPONSE HERE =>',4)
CALL OPENWIND (4,23,24,23,63,0,4+112)
DO WHILE (.NOT.DONE)
CALL CLR(4)
CALL LOCATEW (4,0,0)
CALL AREAD(BIGCHAR,ILEN)
CALL CTOS(BIGCHAR,IDCH1)
ILF=LEFT$(IDCH1,1)
CALL STOC(ILF,C1)
DO X = 1, 5
ISPACE(X)=0
END DO
IF ((C1.EQ.'E').AND.(ILEN.EQ.1)) THEN
DONE=.TRUE.
ELSE IF ((C1.LT.'0').OR.(C1.GT.'9')) THEN
CALL BEEP
CALL BEEP
ELSE
Y=0
DO X = 1, ILEN
IMID=MID$(IDCH1,1,X)
CALL STOC(IMID,C1)
IF ((C1.EQ.' ').AND.(Y.LT.4)) THEN
Y=Y+1
ISPACE(Y)=X
END IF
END DO
IF ((Y.EQ.1).OR.(Y.EQ.3)) THEN
ISPACE(Y+1)=ILEN+1
DO X = 1, Y+1
CLIST2(X)=' '
IMID=MID$(IDCH1,(ISPACE(X)-ISPACE(X-1)-1),(ISPACE(X-1)+1))
CALL STOC(IMID,CLIST2(X))
END DO
IERR=0
DVAL=VAL(CLIST2(1))
IERR=IERR+ISERROR()
IF (IERR.EQ.0) I=INT(DVAL)
DO X = 2, Y+1
DVAL=VAL(CLIST2(X))
IERR=IERR+ISERROR()
END DO

```

```

IF (IERR.EQ.0) THEN
II=0
IF (Y.EQ.1) THEN
DO X = 1, 3
IF (LOOP(X).EQ.1) II=X
END DO
IF (II.NE.0) THEN
DO X = II, LOOP(0)-1
RLOOP(X,1)=RLOOP((X+1),1)
RLOOP(X,2)=RLOOP((X+1),2)
RLOOP(X,3)=RLOOP((X+1),3)
LOOP(X)=LOOP(X+1)
END DO
LOOP(0)=LOOP(0)-1
Y=99
END IF
END IF
IF (Y.EQ.3) THEN
A1=VAL(CLIST2(2))
A2=VAL(CLIST2(3))
A3=VAL(CLIST2(4))
DO X = 1, 3
IF (LOOP(X).EQ.1) II=X
END DO
IF((II.EQ.0).AND.(LOOP(0).LT.3)) THEN
II=LOOP(0)+1
LOOP(0)=LOOP(0)+1
END IF
IF ((II.NE.0).AND.(A3.NE.0.0)) THEN
LOOP(II)=I
RLOOP(II,1)=A1
RLOOP(II,2)=A3
RLOOP(II,3)=1+NINT(ABS(A2-A1)/A3)
A2=A1+(RLOOP(II,3)-1)*A3
ELSE
CALL BEEP
IERR=86
END IF
END IF
IF (IERR.NE.86) THEN
SELECT CASE (I)
CASE (1:4)
PARM(I)=VAL(CLIST2(2))
WRITE(C8,'(F8.3)')PARM(I)
CALL BLDB(1,(I+1),36,C8,4)

```

```

IF (Y.EQ.3) THEN
WRITE(C8,'(F8.3)')A2
WRITE(C3,'(I3)')INT(RLOOP(II,3))
CALL BLDB(2,(I+1),1,C8//' : '//C3,4)
END IF
IF (Y.EQ.99) CALL BLDB(2,(I+1),1,'      ',4)
CASE (5:11,14)
PARM(I)=VAL(CLIST2(2))
WRITE(C8,'(F8.3)')PARM(I)
CALL BLDB(1,(I+2),36,C8,4)
IF (Y.EQ.3) THEN
WRITE(C8,'(F8.3)')A2
WRITE(C3,'(I3)')INT(RLOOP(II,3))
CALL BLDB(2,(I+2),1,C8//' : '//C3,4)
END IF
IF (Y.EQ.99) CALL BLDB(2,(I+2),1,'      ',4)
CASE (12:13)
PARM(I)=INT(VAL(CLIST2(2)))
II=INT(PARM(I))
WRITE(C8,'(I4)')II
CALL BLDB(1,(I+2),36,C8,4)
IF (Y.EQ.3) THEN
WRITE(C8,'(I4)')INT(A2)
WRITE(C3,'(I3)')INT(RLOOP(II,3))
CALL BLDB(2,(I+2),1,C8//' : '//C3,4)
END IF
IF (Y.EQ.99) CALL BLDB(2,(I+2),1,'      ',4)
CASE DEFAULT
CALL BEEP
END SELECT
END IF
ELSE
CALL BEEP
END IF
ELSE
CALL BEEP
END IF
END DO ! (END of do while)
DONE=.FALSE.
*
* (CHECK IF DATA WILL FIT WITHIN ALLOTTED RUN NUMBERS
AVAILABLE)
X=RLOOP(3,3)*RLOOP(2,3)*RLOOP(1,3)
IF ((FILEDATA).AND.(X.GT.99)) THEN

```

```

CALL CLS
CALL OPENWIND(10,8,18,15,61,3,4+112)
CALL TITLE(10,'PROGRAM TERMINATED',0,0,4+112)
CALL CLRB(10)
CALL BLDB (10,1,1,'RUN # 99    EXCEEDED FOR SPECIFIED
ARRAYS',116)
CALL BLDB (10,2,1,'PRESS ANY KEY TO EXIT TO DOS SCREEN
THEN',116)
CALL BLDB (10,3,1,'RESTART PROGRAM    & SELECT NEW
PARAMETERS',116)
CALL CUROFF
CALL TONE(440,50)
CALL ANYKEY
CALL CURON
CALL CLS
STOP
END IF
*
* (INSERT MAJOR LOOP HERE)
IC=0
DO WHILE (IC.NE.INT(RLOOP(3,3)))
IB=0
IC=IC+1
IF (LOOP(3).NE.0) PARM(LOOP(3))=RLOOP(3,1)+(IC-1)*RLOOP(3,2)
DO WHILE (IB.NE.INT(RLOOP(2,3)))
IA=0
IB=IB+1
IF (LOOP(2).NE.0) PARM(LOOP(2))=RLOOP(2,1)+(IB-1)*RLOOP(2,2)
DO WHILE (IA.NE.INT(RLOOP(1,3)))
IA=IA+1
IF (LOOP(1).NE.0) PARM(LOOP(1))=RLOOP(1,1)+(IA-1)*RLOOP(1,2)
DONE=.FALSE.
*
PA=PARM(1)
QA=PARM(2)
TA=PARM(3)
CPA=PARM(4)
RHOA=PA*144.0*28.97/1545.0/(TA+460.0)
KS=PARM(5)
RHOS=PARM(6)
CPS=PARM(7)
TS=PARM(8)
TDIFF=PARM(9)
HS=PARM(10)
HC=PARM(11)

```



```

M=INT(PARM(12))
MM=M+1
N=INT(PARM(13))
NN=N+1
DR=PARM(14)
DZ=HS/2.0/N
TIMENG=99999
TIMEZB=99999

```

*

* (SET VARIABLES WHICH ARE CONSTANT DURING NUMERICAL COMPUTATION LOOP)

```

SUM=0.0
APV=6.5183
BPV=1018.6
CPV=192.7
MA=29.0
MB=131.39
RW=0.25
HFG=0.103
EQ1(1)=APV-BPV/(TS+CPV)
PV1(1)=EXP(EQ1(1))/760.
MOL(1)=PV1(1)*14.7/PA
EFFMASS(1)=MOL(1)*MB+(1.-MOL(1))*MA
MFE(1)=MOL(1)*MB/EFFMASS(1)
DO X = 0, MM
H(X)=0.65/HC
MFG(X)=MFE(1)
G(X)=10.5
A(X)=2.0*PI*DR*(RW+X*DR)
TG(X)=TS
M1(X)=0.1
DO Y = 0, NN
T(X,Y)= TS
TT(X,Y)=TS
END DO
END DO
A(0)=PI*DR*(RW+DR/4.0)
TG(0)=TA
DO X = 1, INDEX
DO Y = 1, IOUTMAX
VOL(X,Y)=0.0
REFF(X,Y)=0.0
END DO
END DO

```

*

```

* (CHECK TIME INCREMENT FOR NUMERICAL STABILITY)
  DTIME=RHOS*CPS*60.0/2.0/(H(0)/DZ+KS/DR/DR+KS/DZ/DZ)
*   ! DTIME IS THE MAX TIME (min) FOR STABILITY
  STABLE=.FALSE.
  DT=1E-4 !(time step in minutes)
  DO WHILE (.NOT.STABLE)
  IF (DT.GT.DTIME) THEN
  IF (DTIME.GT.DT/2.0) THEN
  DT=DT/2.0
  ELSE
  DT=DT/10
  END IF
  END IF
  IF (DTIME.GT.DT) STABLE=.TRUE.
  END DO
  PARM(15)=DT
  DT=DT/60.0 !(time step in hours)
  PARM(16)=DTIME
*
* (SET CODE VALUES TO ID DATA LABELING)
  COUNT=1
  WRITE(COUNTS,'(I2.2)')COUNT
  FN=COUNTS
  W=0
*
* (SET UP BASE FILE WITH PARAMETER VALUES)
  IF (FILEDATA) THEN
  FULLFNAME=FPATH//PREFNAME//FNUM//'00.HOT'
  OPEN (5,FILE=FULLFNAME)
  WRITE(5,'(16F8.3)') (PARM(X),X=1,16)
  WRITE(5,'(I2)') CMAX,COUNT
  WRITE(5,'(F8.3)') (TIME(X),X=1,CMAX)
  DO X = 1, INDEX
  DO Y = 1, CMAX
  WRITE(5,'(2F8.3)') VOL(X,Y),REFF(X,Y)
  END DO
  END DO
  CLOSE (5)
  END IF
*
* (SET PAGE ONE PRINTOUT WITH PARAMETER VALUES)
  IF (PRTRESULTS) THEN
  OPEN (1,FILE='PRN')
  WRITE(1,*) ' ',WTITLE,': ',PREFNAME,FNUM,'00'
  C8=DAT()

```

```

C11=CLK()
WRITE(1,*) ' DATE = ',C8,' CLOCK = ',C11
WRITE(1,*)
WRITE(1,*) ' GAS STREAM PARAMETERS'
WRITE(1,'(5X,A33,F8.3,A5)')' 1-Pressure .....',
&PARM(1),' psia'
WRITE(1,'(5X,A33,F8.3,A4)')' 2-Fracture flow rate .....',
&PARM(2),' cfm'
WRITE(1,'(5X,A33,F8.3,A2)')' 3-Temperature .....',
&PARM(3),' F'
WRITE(1,'(5X,A33,F8.3,A10)')' 4-Heat capacity .....',
&PARM(4),' Btu/lbm/F'
WRITE(1,*) ' ROCK ZONE PARAMETERS'
WRITE(1,'(5X,A33,F8.3,A12)')' 5-Thermal conductivity .....',
&PARM(5),' Btu/hr/ft/F'
WRITE(1,'(5X,A33,F8.3,A9)')' 6-Density .....',
&PARM(6),' lbm/ft^3'
WRITE(1,'(5X,A33,F8.3,A10)')' 7-Heat capacity .....',
&PARM(7),' Btu/lbm/F'
WRITE(1,'(5X,A33,F8.3,A2)')' 8-Initial temperature .....',
&PARM(8),' F'
WRITE(1,'(5X,A33,F8.3,A2)')' 9-Target temperature increase ..',
&PARM(9),' F'
WRITE(1,'(4X,A34,F8.3,A3)')' 10-Crack separation .....',
&PARM(10),' ft'
WRITE(1,'(4X,A34,F8.3,A3)')' 11-Crack width .....',
&PARM(11),' in'
WRITE(1,'(4X,A34,I4)')' 12-Radial nodes (max 100) .....',
&INT(PARM(12))
WRITE(1,'(4X,A34,I4)')' 13-Axial nodes (max 100).....',
&INT(PARM(13))
WRITE(1,'(4X,A34,F8.3,A3)')' 14-Radial increment .....',
&PARM(14),' ft'
WRITE(1,'(4X,A34,F8.3,A4)')' 15-Time increment used .....',
&PARM(15),' min'
WRITE(1,'(4X,A34,F8.3,A4)')' 16-Max time increment allowed .....',
&PARM(16),' min'
WRITE(1,*)
WRITE(1,*) ' Radial spread and volume affected not available'
&/' at this time'
WRITE(1,'(A)') '1'
CLOSE (1)
END IF

```

*

* (NEW SCREEN PRIOR TO COMPUTATIONAL LOOP)

```

CALL CLS
CALL OPENWIND (1,0,0,22,58,3,1+8)
CALL TITLE (1,'SUBSURFACE AND HOT GAS PARAMETERS ..
'//PREFNAME//
&FNUM,0,0,1+8)
CALL CLR(1)
CALL OPENWIND (2,23,0,23,79,0,6)
CALL CLR(2)
CALL LOCATEW (1,0,0)
CALL BLDB(1,1,1,'GAS STREAM PARAMETERS',9)
WRITE (C8,'(F8.3)') PARM(1)
CALL BLDB(1,2,1,' 1-Pressure ..... '//C8// ' psia'
&,9)
WRITE (C8,'(F8.3)') PARM(2)
CALL BLDB(1,3,1,' 2-Fracture flow rate ..... '//C8// ' cfm',9)
WRITE (C8,'(F8.3)') PARM(3)
CALL BLDB(1,4,1,' 3-Temperature ..... '//C8// ' F',9)
WRITE (C8,'(F8.3)') PARM(4)
CALL BLDB(1,5,1,' 4-Heat capacity ..... '//C8//
&' Btu/lbm/F',9)
CALL BLDB(1,6,1,'ROCK ZONE PARAMETERS',9)
WRITE (C8,'(F8.3)') PARM(5)
CALL BLDB(1,7,1,' 5-Thermal conductivity ..... '//C8//
&' Btu/hr/ft/F',9)
WRITE (C8,'(F8.3)') PARM(6)
CALL BLDB(1,8,1,' 6-Density ..... '//C8//
&' lbm/ft^3',9)
WRITE (C8,'(F8.3)') PARM(7)
CALL BLDB(1,9,1,' 7-Heat capacity ..... '//C8//
&' Btu/lbm/F',9)
WRITE (C8,'(F8.3)') PARM(8)
CALL BLDB(1,10,1,' 8-Initial temperature ..... '//C8// ' F',9)
WRITE (C8,'(F8.3)') PARM(9)
CALL BLDB(1,11,1,' 9-Target temperature increase .. '//C8// ' F',9)
WRITE (C8,'(F8.3)') PARM(10)
CALL BLDB(1,12,1,'10-Crack separation ..... '//C8// ' ft',9)
WRITE (C8,'(F8.3)') PARM(11)
CALL BLDB(1,13,1,'11-Crack width ..... '//C8// ' in',9)
WRITE (C4,'(I4)') INT(PARM(12))
CALL BLDB(1,14,1,'12-Radial nodes (max 100) ..... '//C4,9)
WRITE (C4,'(I4)') INT(PARM(13))
CALL BLDB(1,15,1,'13-Axial nodes (max 100)..... '//C4,9)
WRITE (C8,'(F8.3)') PARM(14)
CALL BLDB(1,16,1,'14-Radial increment ..... '//C8// ' ft',9)
WRITE (C8,'(F8.3)') PARM(15)

```

```

CALL BLDB(1,17,1,'15-Time increment used ..... '//C8//' min'
&,9)
WRITE (C8,'(F8.3)') PARM(16)
CALL BLDB(1,18,1,'16-Max time increment allowed ... '//C8//' min'
&,9)
CALL BLDB(2,0,1,'Time since start of gas injection'//
&' (day:hour:min)',6)
*
* (THIS IS THE MAJOR NUMERICAL COMPUTATION LOOP)
CALL CUROFF
OPEN (15,FILE='TEMP.DAT',STATUS='UNKNOWN')
DO WHILE ((.NOT.DONE).AND.(STABLE))
W=W+1
RUNTIME=W*DT*60.0
NLIM=INT(RUNTIME)
MLIM=MOD(NLIM,1440)
WRITE (D$,'(I2)') NLIM/1440
WRITE (H$,'(I2)') MLIM/60
WRITE (M$,'(I2)') MOD(MLIM,60)
CALL BLDB(2,0,50,D$//':'//H$//':'//M$,6)
Q=H(0)*A(0)*(TG(0)-T(0,0))
A1=2.0*H(0)*DT/RHOS/CPS/DZ
A2=KS*DT/RHOS/CPS/DR/DR/(RW+DR/4.0)
A3=KS*DT/RHOS/CPS/DZ/DZ
A4=RW+DR/2.0
TT(0,0)=A1*(TG(0)-T(0,0))+A2*(T(1,0)-T(0,0))+A3*(T(0,1)-
&T(0,0))*2.0+T(0,0)
DO Y = 1, N
TT(0,Y)=A3*(T(0,Y-1)+T(0,Y+1)-2.0*T(0,Y))+A2*A4*(T(1,Y)-T(0,Y))+
&T(0,Y)
END DO
TT(0,N+1)=TT(0,N-1)
SPENT=.FALSE.
DO X = 1, M
IF (.NOT. SPENT) THEN
TG(X)=TG(X-1)-2.0*Q/(QA*60.0*RHOA*CPA)
Q=H(X)*A(X)*(TG(X)-T(X,0))
IF (TG(X).LE.T(X,0)) THEN
TG(X)=T(X,0)
Q=QA*60.0*RHOA*CPA*(TG(X-1)-TG(X))/2.0
END IF
IF (TG(X).LE.TS) THEN
SPENT=.TRUE.
TG(X)=TS
END IF

```

```

A1=2.0*DT/RHOS/CPS/DZ/A(X)
A5=KS*DT/RHOS/CPS/DR/DR/(RW+X*DR)
A6=RW+X*DR+DR/2.0
A7=RW+X*DR-DR/2.0
TT(X,0)=A1*Q+A5*(T(X+1,0)-T(X,0))*A6/2.0
TT(X,0)=TT(X,0)+A5*A7*(T(X-1,0)-T(X,0))/2.0
TT(X,0)=TT(X,0)+A3*2.0*(T(X,1)-T(X,0))+T(X,0)
+   -A1*HFG
DO Y = 1, N
TT(X,Y)=A3*(T(X,Y-1)+T(X,Y+1)-2.0*T(X,Y))+T(X,Y)
TT(X,Y)=TT(X,Y)+A5*A6*(T(X+1,Y)-T(X,Y))/2.0
TT(X,Y)=TT(X,Y)+A5*A7*(T(X-1,Y)-T(X,Y))/2.0
END DO
TT(X,N+1)=TT(X,N-1)
END IF

```

* REAL ARRAY VARIABLES

```

* ! MIN(X): MASS OF CONTAMINANT ENTERING THE NODE, lbs
* ! MOUT(X): MASS OF CONTAMINANT LEAVING THE NODE, lbs
* ! MI(X): MASS OF CONTAMINANT PRESENT INITIALLY, lbs
* ! MFG(X): MASS FRACTION OF CONTAMINANT IN GAS
* ! MOL(X): MOLE FRACTION
* ! MFE(X): EQUILIBRIUM MASS FRACTION AT BOUNDARY LAYER
* ! MDOT(X): MASS TRANSPORTED INTO THE GAS, lbs
* ! MLS(X): MASS LEFT AT THE SURFACE, lbs
* ! MNEW(X): NEW MASS IN THE ith CELL, lbs
* ! VI(X): VOLUME OF THE ith CELL, ft^3
* ! PV1(X): VAPOR PRESSURE OF THE CONTAMINANT, atm
* ! BV(X): DRIVING FORCE

```

```

MIN(X)=RHOA*QA*60.0*DT*MFG(X-1)
MOUT(X)=RHOA*QA*60.0*DT*MFG(X)
VI(X)=A(X)*HC/12.0
MI(X)=RHOA*VI(X)*MFG(X)
* MFG(X)=(MI(X)+MIN(X)-MOUT(X))/RHOA/VI(X)
EQ1(X)=APV-BPV/(TT(X,0)+CPV)
PV1(X)=(EXP(EQ1(X)))/760.0
MOL(X)=PV1(X)*14.7/PA
EFFMASS(X)=MOL(X)*MB+(1-MOL(X))*MA
MFE(X)=MOL(X)*MB/EFFMASS(X)
BV(X)=MFE(X)-MFG(X)
R=2.0*G(X)*A(X)/RHOA/VI(X)
FAC(X)=1.0-EXP(-R*DT)
MDOT(X)=RHOA*VI(X)*FAC(X)*BV(X)
MLS(X)=M1(X)*A(X)

```

```

IF (MDOT(X).GT.MLS(X)) THEN
MDOT(X)=MLS(X)
END IF
M1(X)=M1(X)-MDOT(X)/A(X)
MNEW(X)=MI(X)+MIN(X)-MOUT(X)+MDOT(X)
MFG(X)=MNEW(X)/RHOA/VI(X)
IF (MOD(W,600000).EQ.0) THEN
WRITE(15,*)'*****X=',X,' M=',M
WRITE(15,*) MIN(X), MOUT(X), VI(X)
WRITE(15,*) EQ1(X), PV1(X), MOL(X)
WRITE(15,*) EFFMASS(X), MFE(X), BV(X)
WRITE(15,*) MDOT(X), MI(X), MNEW(X)
WRITE(15,*) MFG(X), MLS(X), M1(X)
WRITE(15,*) TT(X,0), T(X,0), TG(X)
END IF
QIN(X)=H(X)*A(X)*(TG(X)-T(X,0))+KS*A(X)*(T(X,1)-T(X,0))/DZ-HFG
QROCK(X)=RHOS*CPS*A(X)*(DZ/2.0)*(TT(X,0)-T(X,0))/DT
QOUT(X)=-KS*PI*(RW+X*DR+DR/2.0)*(DZ/2.0)*(T(X+1,0)-T(X,0))/DR
+ -KS*PI*(RW+X*DR-DR/2.0)*(DZ/2.0)*(T(X-1,0)-T(X,0))/DR
END DO
SUM=SUM+MFG(M)
TF=TG(M)-2.0*Q/(QA*60.0*RHOA*CPA)
IF (SPENT) TF=TS
SPENT=.FALSE.
DO X = 0, M+1
DO Y = 0, N+1
T(X,Y)=TT(X,Y) !(reset new to old)
END DO
END DO
IF (TIMENG.EQ.99999) THEN
IF (TT(M,0).GT.(TS+5)) TIMENG=RUNTIME
END IF
IF (RUNTIME.GE.TIME(COUNT)) DATAOUT=.TRUE.
IF (TIMEZB.EQ.99999) THEN
IF (TT(1,N).GT.(TS+5)) TIMEZB=RUNTIME
END IF
*
* (PREPARE FOR DATA OUT OF RADIAL AND VOLUMETRIC SPREAD OF
TEMPERATURE)
IF (DATAOUT) THEN
DO Z = 1, INDEX
TEFF=TS+FLOAT(Z)*TDIFF
DO X = 0, M
Y=0
Q=0.0

```

```

DO Y = 0, N
IF (TT(X, Y).LT.TEFF) EXIT
END DO
IF ((Y.LT.NN).AND.(Y.GT.0)) Q=FLOAT(Y-1)+
&(TEFF-TT(X, Y-1))/(TT(X, Y)-TT(X, Y-1))
IF (Y.EQ.NN) Q=N
VOL(Z, COUNT)=VOL(Z, COUNT)+2.0*A(X)*Q*DZ
END DO
X=0
Q=0.0
DO X = 0, M
IF (TT(X, 0).LT.TEFF) EXIT
END DO
IF ((X.LT.MM).AND.(X.GT.0)) Q=FLOAT(X-1)+
&(TEFF-TT(X-1, 0))/(TT(X, 0)-TT(X-1, 0))
IF (X.EQ.MM) Q=M
REFF(Z, COUNT)=Q*DR
END DO !(End of Z loop)
END IF !(End of dataout)
*
* (SEND RESULTS TO DISK STORAGE FOR LATER ACQUISITION)
IF (DATAOUT.AND.FILEDATA) THEN
FULLFNAME=FPATH//PREFNAME//FNUM//FN//'.HOT'
OPEN (4, FILE=FULLFNAME)
WRITE(4, '(2F8.3)') RUNTIME, TF
WRITE(4, '(2I3)') M, N
DO Y = 0, N
WRITE(4, '(10F8.3)') (TT(X, Y), X=0, M)
END DO
DO X = 1, M
WRITE(4, '(F8.3, 4X, 5F10.4, 10(/, 12X, 5F10.4))')
+ TG(X), MDOT(X)
WRITE(4, '(10(/, 12X, 5F10.8))') MFG(X)
WRITE(4, '(10(/, 12X, 5F10.8))') MLS(X)
WRITE(4, '(10(/, 12X, 5F10.8))') M1(X)
WRITE(4, '(10(/, 12X, 5F10.4))') SUM
WRITE(4, '(F8.3, 4X, F8.3, 4X, F8.3)') QIN(X),
+ QROCK(X), QOUT(X)
END DO
CLOSE(4)
FULLFNAME=FPATH//PREFNAME//FNUM//'00.HOT'
OPEN (5, FILE=FULLFNAME)
WRITE(5, '(16F8.3)') (PARM(X), X=1, 16)
WRITE(5, '(I2)') CMAX, COUNT
WRITE(5, '(F8.3)') (TIME(X), X=1, CMAX)

```



```

DO X = 1, INDEX
DO Y = 1, CMAX
WRITE(5,'(2F8.3)') VOL(X,Y),REFF(X,Y)
END DO
END DO
CLOSE (5)
END IF ! (End of filing results)
*
* (SEND RESULTS TO PRINTER FOR HARD COPY)
IF (DATAOUT.AND.PRTRESULTS) THEN
OPEN (1,FILE='PRN')
WRITE(1,*) ' ',WTITLE,': ',PREFNAME,FNUM,FN
C8=DAT()
C11=CLK()
WRITE(1,*) ' DATE = ',C8,' CLOCK = ',C11
NLIM=INT(RUNTIME)
MLIM=MOD(NLIM,1440)
WRITE(D$,'(I2)') NLIM/1440
WRITE(H$,'(I2)') MLIM/60
WRITE(M$,'(I2)') MOD(MLIM,60)
WRITE(1,*) ' Time since start of gas injection (day:hour:min) '
&//D$//':://H$//':://M$
WRITE(1,'(A38,I8)') ' Injected gas exit temperature (F) ',
&NINT(TA)
WRITE(1,'(A65)') ' R(ft) <-----Z = distance from crack'//
&' surface (ft)----->'
IF (N.LT.11) THEN
NLIM=N
ELSE
NLIM=10
END IF
WRITE(1,'(A10)') ' '
DO Y = 0, NLIM
WRITE(1,'(A,F5.2)') '&',DZ*Y
END DO
WRITE(1,'(A65)') ' -----'
&//'-----'
IF (M.LT.46) THEN
MLIM=M
ELSE
MLIM=45
ENDIF
DO X = 0, MLIM
WRITE(1,'(A4,F4.1,A2)') ' ',X*DR,' '
DO Y = 0, NLIM

```

```

WRITE(1,'(A,I5)') '&',NINT(TT(X,Y))
END DO
END DO
WRITE(1,'(A19)') '  Rock temp rise '
DO X = 1, INDEX
WRITE(1,'(A1,I8)') '&:',INT(X*TDIFF)
END DO
WRITE(1,'(A5)') '& (F)'
WRITE(1,'(A19)') '  Volume of rock '
DO X = 1, INDEX
WRITE(1,'(A1,F8.1)') '&:',VOL(X,COUNT)
END DO
WRITE(1,'(A8)') '& (ft^3)'
WRITE(1,'(A19)') '  Radial spread '
DO X = 1, INDEX
WRITE(1,'(A1,F8.1)') '&:',REFF(X,COUNT)
END DO
WRITE(1,'(A6)') '& (ft)'
WRITE(1,'(A)') '1'
CLOSE (1)
END IF !(end of printing results)
*
* (IF PRINTER AND DISK OUTPUT IS NOT SELECTED DISPLAY T vs
DISTANCE)
  IF (.NOT.SUMMARY) THEN
    IF ((.NOT.PRTRESULTS).AND.(.NOT.FILEDATA).AND.(DATAOUT))
THEN
    CALL CLRW(1)
    CALL BLDB(1,0,0,'Radius(ft)  WallTemp(F) '//
&'  Radius(ft)  WallTemp(F)',1+8)
    MLIM = 39
    IF (M.LT.39) MLIM=M
    IF (-1**MLIM.GT.0) MLIM=MLIM-1
    MLIM = MLIM/2
    DO X = 0, MLIM
    WRITE(C4,'(F4.1)') X*DR
    WRITE(C5,'(I5)') NINT(TT(X,0))
    CALL BLDB(1,X+1,3,C4//'      '//C5,1+8)
    WRITE(C4,'(F4.1)') (X+1+MLIM)*DR
    WRITE(C5,'(I5)') NINT(TT((X+1+MLIM),0))
    CALL BLDB(1,X+1,32,C4//'      '//C5,1+8)
    END DO
    END IF
    END IF
*

```

```

* (UPDATE INFORMATION CONTROLLING OUTPUT OF DATA)
  IF (DATAOUT) THEN
    COUNT=COUNT+1
    DATAOUT=.FALSE.
    IF (COUNT.GT.CMAX) THEN
      DONE=.TRUE.
    ELSE
      WRITE(COUNTS,'(I2.2)')COUNT
      FN=COUNTS
    END IF
  END IF !(end of update)
*
  END DO !(end while loop)
  CALL CURON
*
* (PRINTOUT A NEW PAGE ONE WITH VOL AND RADIUS DATA)
  IF ((PRTRESULTS).OR.(SUMMARY)) THEN
    OPEN (1,FILE='PRN')
    WRITE(1,*) ' ',WTITLE,': ',PREFNAME,FNUM,'00'
    C8=DAT()
    C11=CLK()
    WRITE(1,*) ' DATE = ',C8,' CLOCK = ',C11
    WRITE(1,*)
    WRITE(1,*) ' GAS STREAM PARAMETERS'
    WRITE(1,'(5X,A33,F8.3,A5)')' 1-Pessure .....',
    &PARM(1),' psia'
    WRITE(1,'(5X,A33,F8.3,A4)')' 2-Fracture flow rate .....',
    &PARM(2),' cfm'
    WRITE(1,'(5X,A33,F8.3,A2)')' 3-Temperature .....',
    &PARM(3),' F'
    WRITE(1,'(5X,A33,F8.3,A10)')' 4-Heat capacity .....',
    &PARM(4),' Btu/lbm/F'
    WRITE(1,*) ' ROCK ZONE PARAMETERS'
    WRITE(1,'(5X,A33,F8.3,A12)')' 5-Thermal conductivity .....',
    &PARM(5),' Btu/hr/ft/F'
    WRITE(1,'(5X,A33,F8.3,A9)')' 6-Density .....',
    &PARM(6),' lbm/ft^3'
    WRITE(1,'(5X,A33,F8.3,A10)')' 7-Heat capacity .....',
    &PARM(7),' Btu/lbm/F'
    WRITE(1,'(5X,A33,F8.3,A2)')' 8-Initial temperature .....',
    &PARM(8),' F'
    WRITE(1,'(5X,A33,F8.3,A2)')' 9-Target temperature increase ..',
    &PARM(9),' F'
    WRITE(1,'(4X,A34,F8.3,A3)')' 10-Crack separation .....',
    &PARM(10),' ft'

```

```

WRITE(1,'(4X,A34,F8.3,A3)')' 11-Crack width .....',
&PARM(11),' in'
WRITE(1,'(4X,A34,I4)')' 12-Radial nodes (max 100) .....',
&INT(PARM(12))
WRITE(1,'(4X,A34,I4)')' 13-Axial nodes (max 100).....',
&INT(PARM(13))
WRITE(1,'(4X,A34,F8.3,A3)')' 14-Radial increment .....',
&PARM(14),' ft'
WRITE(1,'(4X,A34,F8.3,A4)')' 15-Time increment used .....',
&PARM(15),' min'
WRITE(1,'(4X,A34,F8.3,A4)')' 16-Max time increment allowed .....',
&PARM(16),' min'
IF (TIMEZB.NE.99999) THEN
NLIM=INT(TIMEZB)
MLIM=MOD(NLIM,1440)
WRITE(1,'(4X,A34)')' **-Axial spread sensed after ..... '
WRITE(1,'(A,I2,A,I2,A,I2,A9)')'&','NLIM/1440,':',MLIM/60,':',
&MOD(MLIM,60),' dd/hh/mm'
END IF
IF (TIMENG.NE.99999) THEN
NLIM=INT(TIMENG)
MLIM=MOD(NLIM,1440)
WRITE(1,'(4X,A34)')' **-Results suspect after ..... '
WRITE(1,'(A,I2,A,I2,A,I2,A9)')'&','NLIM/1440,':',MLIM/60,':',
&MOD(MLIM,60),' dd/hh/mm'
END IF
WRITE(1,*)
WRITE(1,*)' Time Spread (ft) at delta T of'//
&' Volume (ft^3) at delta T of'
WRITE(CCC2,'(I2)')INT(TDIFF)
WRITE(CC2,'(I2)')INT(2*TDIFF)
WRITE(C2,'(I2)')INT(3*TDIFF)
WRITE(1,*)' day:hr:min ...'//CCC2//'F.....'//CC2//'F.....'//
&C2//'F... '//' ...'//CCC2//'F.....'//CC2//'F.....'//C2//'F...'
DO X = 1, CMAX
NLIM=INT(TIME(X))
MLIM=MOD(NLIM,1440)
WRITE(1,'(5X,A,I2,A,I2,A,I2,A)')' ',NLIM/1440,':',MLIM/60,':',
&MOD(MLIM,60),' '
DO Y = 1, INDEX
WRITE(1,'(A,F8.1)') '&',REFF(Y,X)
END DO
WRITE(1,'(A5)') '&'
DO Y = 1, INDEX
WRITE(1,'(A,F8.1)') '&',VOL(Y,X)

```

```
END DO
END DO
WRITE(1,'(A)') '1'
CLOSE (1)
END IF
*
* (PROVIDE INFORMATION CONTROL FOR MASTER LGOPS)
  IRUN=IRUN+1
  IF (IRUN.GT.99) THEN
    WRITE(1,*)'Maximum run number exceeded.. program stop'
    STOP
  END IF
  WRITE(FNUM,'(I2.2)')IRUN
*
* (INSERT END OF MASTER LOOP(S) HERE)
  END DO !(END LOOP A)
  END DO !(END LOOP B)
  END DO !(END LOOP C)
*
*
  CALL CLRW(2)
  CALL UNTITLE(1)
  CALL FILLB(1)
  CALL BLDB (1,9,20,'THATS ALL FOLKS',1+8+128)
  CALL CUROFF
  DO X = 500, 900, 200
  CALL TONE (X,X/10)
  END DO
  CALL ANYKEY
  CALL CURON
  CALL CLS
  END !(END OF PROGRAM)
```

APPENDIX-B

DERIVATION OF EQUATIONS

1. R-NODE 0, Z-NODE 0

$$q_s + k\pi \left(r_w + \frac{\Delta r}{4}\right) \left(\frac{\Delta z}{2}\right) \left(\frac{T_{1,0} - T_{0,0}}{\Delta r}\right) + k\pi \Delta r \left(r_w + \frac{\Delta r}{4}\right) \left(\frac{T_{0,1} - T_{0,0}}{\Delta z}\right) =$$

$$\rho c_p \pi \Delta r \left(r_w + \frac{\Delta r}{4}\right) \cdot \frac{\Delta z}{2} \cdot \frac{(T_{0,0}^{\tau} - T_{0,0})}{\Delta t}$$

Rearranging,

$$T_{0,0}^{\tau} = T_{0,0} + \frac{2h\Delta t}{\rho c_p \Delta z} (T_{s0} - T_{0,0}) + \frac{k\Delta t (T_{1,0} - T_{0,0})}{\rho c_p \Delta r^2 \left(r_w + \frac{\Delta r}{4}\right)} + \frac{2k\Delta t}{\rho c_p \Delta z^2} (T_{0,1} - T_{0,0})$$

Considering only the terms for node (0,0) we get,

$$T_{0,0}^{\tau} = T_{0,0} + \frac{2h\Delta t}{\rho c_p \Delta z} T_{0,0} + \frac{k \left(r_w + \frac{\Delta r}{2}\right) \Delta t}{\rho c_p \Delta r^2 \left(r_w + \frac{\Delta r}{4}\right)} T_{0,0} - \frac{2k\Delta t}{\rho c_p \Delta z^2} T_{0,0}$$

Rearranging for Stability,

$$\Delta t < \frac{\rho c_p}{\frac{2h}{\Delta z} + \frac{k}{\Delta r^2} \left(\frac{r_w + \frac{\Delta r}{2}}{r_w + \frac{\Delta r}{4}} \right) + \frac{2k}{\Delta z^2}}$$

2. R-NODE 0, Z-NODE j ; j > 0

$$kA(0) \frac{(T_{0,j-1} - T_{0,j})}{\Delta z} + kA(0) \frac{(T_{0,j+1} - T_{0,j})}{\Delta z} + k\pi \left(r_w + \frac{\Delta r}{2} \right) \Delta z \frac{(T_{1,j} - T_{0,j})}{\Delta r}$$

Considering only the terms for node (0,j), we get

$$T_{0,j}^r = T_{0,j} - \frac{k\Delta t}{\rho c_p \Delta z^2} T_{0,j} - \frac{k\Delta t}{\rho c_p \Delta z^2} T_{0,j} - \frac{k\Delta t}{\rho c_p \Delta r^2} \frac{(r_w + \frac{\Delta r}{2})}{\Delta r^2 (r_w + \frac{\Delta r}{4})} T_{0,j}$$

Rearranging for stability

$$\Delta t < \frac{\rho c_p}{\frac{2k}{\Delta z^2} + \frac{k}{\Delta r^2} \frac{(r_w + \frac{\Delta r}{2})}{(r_w + \frac{\Delta r}{4})}}$$

3. R-NODE i , Z-NODE 0

$$\begin{aligned}
 hA(i)(T_{s_i} - T_{i,o}) + k\pi(r_w + i\Delta r + \frac{\Delta r}{2}) \frac{\Delta z}{2} \frac{(T_{i+1,0} - T_{i,0})}{\Delta r} + k\pi(r_w + i\Delta r - \frac{\Delta r}{2}) \frac{\Delta z}{2} \frac{(T_{i-1,0} - T_{i,0})}{\Delta r} \\
 + kA(i) \frac{(T_{i,1} - T_{i,0})}{\Delta z} = \rho C_p A(i) \frac{\Delta z}{2} \frac{(T_{i,0}^* - T_{i,o})}{\Delta t}
 \end{aligned}$$

Rearranging

$$\begin{aligned}
 T_{i,0}^* = T_{i,o} + \frac{2h\Delta t}{\rho c_p \Delta z} (T_{s_i} - T_{i,0}) + \frac{k\Delta t}{2\rho c_p \Delta r^2} \frac{(r_w + i\Delta r + \frac{i\Delta r}{2})}{(r_w + i\Delta r)} (T_{i+1,0} - T_{i,0}) \\
 + \frac{k\Delta t}{2\rho c_p \Delta r^2} \frac{(r_w + i\Delta r - \frac{\Delta r}{2})}{(r_w + i\Delta r)} (T_{i-1,0} - T_{i,0}) + \frac{2k\Delta t}{\rho c_p \Delta z^2} (T_{i,1} - T_{i,0})
 \end{aligned}$$

Considering only those terms for node $(i,0)$, we get

$$\begin{aligned}
 T_{i,0}^* = T_{i,0} - \frac{2h\Delta t}{\rho c_p \Delta z} - \frac{k\Delta t}{2\rho c_p \Delta r^2} \frac{(r_w + i\Delta r + \frac{\Delta r}{2})}{(r_w + i\Delta r)} T_{i,0} - \frac{k\Delta t}{2\rho c_p \Delta r^2} \frac{(r_w + i\Delta r - \frac{\Delta r}{2})}{(r_w + i\Delta r)} - \frac{2k\Delta t}{\rho c_p \Delta z^2} T_{i,0} \\
 = T_{i,0} - \left(\frac{2h\Delta t}{\rho c_p \Delta z} + \frac{k\Delta t}{\rho c_p \Delta r^2} + \frac{2k\Delta t}{\rho c_p \Delta z^2} \right) T_{i,0}
 \end{aligned}$$

Rearranging for Stability,

$$\Delta t < \frac{\rho c_p}{\frac{2h}{\Delta z} + \frac{k}{\Delta r^2} + \frac{2k}{\Delta z^2}}$$

4. R-NODE i, Z-NODE j

$$kA(i) \frac{(T_{i,j-1} - T_{i,j})}{\Delta z} + kA(i) \frac{(T_{i,j+1} - T_{i,j})}{\Delta z} + k\pi(r_w + i\Delta r + \frac{\Delta r}{2}) \Delta z \frac{(T_{i+1,j} - T_{i,j})}{\Delta r}$$

$$+ k\pi(r_w + i\Delta r - \frac{\Delta r}{2}) \Delta z \frac{(T_{i-1,j} - T_{i,j})}{\Delta r} = \rho c_p A(i) \Delta z \frac{(T_{i,j}^x - T_{i,j})}{\Delta t}$$

$$T_{i,j}^x = T_{i,j} - \left(\frac{2k\Delta t}{\rho c_p \Delta z^2} + \frac{k\Delta t}{\rho c_p \Delta r^2} \right) T_{i,j}$$

(or)

$$T_{i,j}^x = T_{i,j} \left(1 - \frac{\Delta t}{\rho c_p} \left(\frac{2k}{\Delta z^2} + \frac{k}{\Delta r^2} \right) \right)$$

Rearranging for stability,

$$\Delta t < \frac{\rho c_p}{\frac{2k}{\Delta z^2} + \frac{k}{\Delta r^2}}$$

DERIVATION OF MASS TRANSPORT EQUATION

Mass of contaminant in any cell 'i' at any time t is given by,

$$m_i = \rho_a V_i MFG(i)$$

Relating the mass fraction of contaminant in gas as a function of time step rather than as a function of the node, we have,

$$(m_i)_t = \rho_a V_i (MFG)_t$$

Between two consecutive time steps, t and t+dt,

$$\frac{dm_i}{dt} = \frac{d(\rho_a V_i MFG)}{dt} = 2g_i a_i (MFE - MFG)$$

Rearranging,

$$\frac{d(MFG)}{dt} = \left(\frac{2g_i a_i}{\rho_a V_i} \right) (MFE - MFG)$$

Let,

$$\frac{2g_i a_i}{\rho_a V_i} = r$$

$$\therefore \frac{d(MFG)}{dt} = r(MFE - MFG)$$

Integrating,

$$\int_t^{(t+dt)} \frac{d(MFG)}{(MFE - MFG)} = \int_t^{(t+dt)} r dt$$

$$-\ln(MFE - MFG) \Big|_t^{t+dt} = r dt$$

$$-\ln(MFE - MFG(t+dt)) + \ln(MFE - MFG(t)) = r dt$$

$$\ln\left(\frac{MFE - MFG(t+dt)}{MFE - MFG(t)}\right) = -r dt$$

$$\frac{MFE - MFG(t+dt)}{MFE - MFG(t)} = e^{-r dt}$$

Rearranging,

$$MFG(t+dt) = MFE(1 - e^{-r dt}) + MFG(t)e^{-r dt}$$

From the initial definition of mass transferred in time dt,

$$\dot{m}_i = \rho_a V_i (MFG(t+dt) - MFG(t))$$

Substituting for $MFG(t+dt)$,

$$\dot{m}_i = \rho_a V_i (MFE (1 - e^{-rdt}) + MFG(t) (e^{-rdt} - 1))$$

Let,

$$fac = (1 - e^{-rdt})$$

Which gives the equation for mass transported as,

$$\dot{m}_i = \rho_a V_i (fac (MFE(i) - MFG(i)))$$

APPENDIX-C

PHYSICAL PROPERTIES OF CONTAMINANTS

Table 1 Important Properties of Commonly Occuring Contaminants

Compound	Molecular Weight	Heat of Vaporization kcal/kg-mol	Vapor Heat Capacity @ 298 K kcal/g-mol K	Heat of Formation kcal/kg-mol	Density g/cm ³	Boiling Point ° C/° F	Viscosity N-s/m
Benzene	78.11	7.352	19.5	30.99	0.8737@ 25° C	80/176	0.649@20° C
Chloroform	119.39	7.08	15.78	-16.76	1.4985@ 15° C	61/142	0.596@15° C
1,1-Dichloroethane	98.96	6.97	18.25	-17.52	1.1757@ 20° C	57.3/135	0.505@25° C
1,1-Dichloroethylene	96.94	6.26	16.02	5.78	1.2129@ 20° C	37/99	0.358@20° C
Methylene Chloride	84.93	6.74	12.19	-16.46	1.3255@ 20° C	40/104	0.449@15° C
1,1,1-Trichloroethane	133.41	7.96	22.07	-18.21	1.3376@ 20° C	114/237	0.903@15° C
1,1,2-Trichloroethylene	131.39	7.52	19.17	4.75	1.4649@ 20° C	87/190	0.566@20° C
Toluene	92.14	7.93	24.73	29.18	0.8660@ 20° C	111/232	0.623@15° C
o-Xylene	106.17	8.8	31.85	29.16	0.8802@ 20° C	144/291	0.809@20° C
Water	18.02	9.717	8.18	-54.6	1.0000@ 4° C	100/212	1.0019@20° C
Hydrogen Chloride	36.46	3.86	6.96	-22.8	1.1870@ -85° C	-85/-121	0.51@-95° C

Table 2 Antoine Constants for Vapor Pressures

Compound	Range, ° c	A	B	C
Benzene	-12 to 3	9.1064	1885.9	244.2
Chloroform	-35 to 61	6.4934	929.44	196.03
1,1-Dichloroethane	-39 to 18	6.9770	1174.02	229.06
1,1-Dichloroethylene	-28 to 32	6.9722	1099.4	237.20
Methylene Chloride	-40 to 40	7.4092	1325.90	252.60
1,1,1-Trichloroethane	-6 to 17	8.6434	2136.6	302.8
1,1,2-Trichloroethylene	18 to 86	6.5183	1018.6	192.7
Toluene	6 to 137	6.9550	1344.8	219.48
o-Xylene	32 to 172	6.9989	1474.68	213.69
Hydrogen Chloride	-	7.17	745.8	258.88

$$\log p = A - \frac{B}{T+C}$$

$$p_v = p/760$$

where p = Vapor Pressure in mm of mercury

T = Temperature in ° c

p_v = Vapor Pressure in atm

A,B,C = Antoine Constants

APPENDIX-D

TRIAL RUN RESULTS

TG = Gas Temperature ; MDOT = Mass Transported ; MFG = Mass Removed ;
MLS = Mass Left at Surface ; QIN = Heat In ; QROCK = Heat Used for Heating
Rock Surface ; QOUT = Heat Leaving.

Runtime Fracture Temperature
1440.000 50.000

Radial Nodes Axial Nodes
45 10

Temperature Distribution - 10 sets (axial) of 45 radial nodes.

612.090 610.993 605.186 596.111 583.860 568.734 554.334 533.703 512.000
490.247 466.270 440.834 414.964 387.924 361.389 335.252 308.585 283.331
258.156 234.533 211.178 188.938 168.353 149.724 133.243 118.413 104.834
92.596 81.423 72.417 65.313 59.529 55.114 52.155 51.620 50.383 50.000
50.000 50.000 50.000 50.000 50.000 50.000 50.000 50.000 50.000

555.804 555.170 549.363 540.288 528.037 512.911 501.911 481.038 459.529
439.482 417.934 394.862 371.984 347.359 324.105 301.385 277.093 255.214
232.389 210.494 189.123 169.042 150.894 134.799 120.866 107.474 95.267 84.439
74.286 67.080 61.461 56.294 52.839 50.772 50.478 50.000 50.000 50.000
50.000 50.000 50.000 50.000 50.000 50.000 50.000 50.000

510.347 509.980 504.173 495.098 482.848 467.722 454.804 433.690 412.374
394.034 374.914 354.207 334.320 312.111 292.138 272.835 250.918 229.967
209.281 189.112 169.727 151.804 136.092 122.533 109.981 97.864 87.029
76.863 68.478 63.071 57.890 53.724 51.228 50.054 50.000 50.000 50.000
50.000 50.000 50.000 50.000 50.000 50.000 50.000 50.000 50.000

470.318 470.106 464.300 455.225 442.974 427.848 413.013 391.658 370.535
353.901 337.211 318.868 301.974 282.179 265.486 249.601 228.986 208.333
188.831 170.389 152.988 137.225 123.949 112.128 100.426 89.583 79.343 70.615
64.000 59.231 54.983 51.818 50.282 50.000 50.000 50.000 50.000 50.000
50.000 50.000 50.000 50.000 50.000 50.000 50.000 50.000

435.672 435.549 429.743 420.668 408.417 393.291 376.539 354.943 334.014
319.086 304.824 288.845 274.943 257.564 244.152 229.101 209.944 189.358
171.039 154.325 138.908 125.304 114.176 103.051 92.200 81.893 72.987 65.697
60.255 56.056 52.740 50.577 50.000 50.000 50.000 50.000 50.000 50.000
50.000 50.000 50.000 50.000 50.000 50.000 50.000 50.000

406.380 406.309 400.502 391.427 379.176 364.050 345.381 323.544 302.808
289.586 277.754 264.139 253.229 238.265 225.475 211.259 193.560 173.041
155.905 140.918 127.486 116.604 105.733 95.304 84.890 75.533 67.959 62.107
56.885 53.545 51.162 50.000 50.000 50.000 50.000 50.000 50.000 50.000
50.000 50.000 50.000 50.000 50.000 50.000 50.000 50.000

382.426 382.384 376.578 367.503 355.252 340.126 319.540 297.461 276.919
265.403 256.000 244.750 234.174 221.625 209.457 196.075 179.834 159.382
143.429 130.170 119.276 110.123 99.728 89.323 78.909 70.501 64.260 59.117
54.179 51.699 50.249 50.000 50.000 50.000 50.000 50.000 50.000 50.000
50.000 50.000 50.000 50.000 50.000 50.000 50.000 50.000

363.801 363.777 357.970 348.896 336.645 321.519 299.015 276.695 256.347
246.537 237.489 229.199 218.674 207.642 196.097 183.550 168.766 148.382
133.612 122.361 113.928 105.471 95.076 84.671 74.257 66.799 61.891 56.791
52.137 50.517 50.000 50.000 50.000 50.000 50.000 50.000 50.000 50.000
50.000 50.000 50.000 50.000 50.000 50.000 50.000 50.000

350.501 350.486 344.679 335.604 323.353 308.228 283.807 261.245 241.091
232.286 226.045 218.908 207.824 196.505 185.396 173.683 160.357 140.040
126.453 115.881 110.494 102.148 91.753 81.348 70.934 64.426 60.230 55.129
50.760 50.000 50.000 50.000 50.000 50.000 50.000 50.000 50.000 50.000
50.000 50.000 50.000 50.000 50.000 50.000 50.000 50.000

342.521 342.511 336.705 327.630 315.379 300.253 273.916 251.112 231.122
224.680 220.064 211.450 200.386 189.355 178.351 167.371 154.606 134.356
123.281 113.317 108.389 100.155 89.760 79.355 68.940 63.382 59.233 54.132
50.048 50.000 50.000 50.000 50.000 50.000 50.000 50.000 50.000 50.000
50.000 50.000 50.000 50.000 50.000 50.000 50.000 50.000

339.862 339.853 334.046 324.971 312.721 297.595 269.928 247.212 227.799
222.686 218.070 209.394 198.329 187.298 176.294 165.314 152.612 132.362
121.439 112.320 107.725 99.490 89.095 78.690 68.276 63.002 58.901 53.800
50.000 50.000 50.000 50.000 50.000 50.000 50.000 50.000 50.000 50.000
50.000 50.000 50.000 50.000 50.000 50.000 50.000 50.000

TG = 698.251 MDOT = 0.0000

MFG = 0.01954072

MLS = 0.00000000

QIN = 42.086 QROCK = 0.000 QOUT = 3.027

TG = 692.376 MDOT = 0.0000

MFG = 0.01954072

MLS = 0.00000000

QIN = 64.548 QROCK = 0.000 QOUT = 4.183

TG = 683.303 MDOT = 0.0000

MFG = 0.01954072

MLS = 0.00000000

QIN = 87.390 QROCK = 0.000 QOUT = 5.720

TG = 671.028 MDOT = 0.0000

MFG = 0.01954072

MLS = 0.00000000

QIN = 109.885 QROCK = 0.000 QOUT = 6.909

TG = 655.555 MDOT = 0.0000

MFG = 0.01954072

MLS = 0.00000000

QIN = 126.918 QROCK = 0.000 QOUT = 2.637

TG = 636.956 MDOT = 0.0000

MFG = 0.01954073

MLS = 0.00000000

QIN = 160.638 QROCK = 0.000 QOUT = 15.051

TG = 616.221 MDOT = 0.0000

MFG = 0.01954073

MLS = 0.00000000

QIN = 174.296 QROCK = 0.000 QOUT = 7.405

TG = 592.482 MDOT = 0.0000

MFG = 0.01954074

MLS = 0.00000000

QIN = 152.565 QROCK = 0.000 QOUT = 5.551

TG = 566.373 MDOT = 0.0000

MFG = 0.01954075

MLS = 0.00000000

QIN = 115.957 QROCK = 0.000 QOUT = 11.205

TG = 538.881 MDOT = 0.0000

MFG = 0.01954076

MLS = 0.00000000

QIN = 125.552 QROCK = 0.000 QOUT = 10.149

TG = 509.992 MDOT = 0.0000

MFG = 0.01954078

MLS = 0.00000000

QIN = 133.767 QROCK = 0.000 QOUT = 7.710

TG = 479.937 MDOT = 0.0000

MFG = 0.01954079

MLS = 0.00000000

QIN = 147.095 QROCK = 0.000 QOUT = 10.386

TG = 449.314 MDOT = 0.0000

MFG = 0.01954079

MLS = 0.00000000

QIN = 152.320 QROCK = 0.000 QOUT = 4.957

TG = 418.125 MDOT = 0.0000

MFG = 0.01954079

MLS = 0.00000000

QIN = 163.136 QROCK = 316.031 QOUT = 5.120

TG = 387.218 MDOT = 0.0000

MFG = 0.01954080

MLS = 0.00000000

QIN = 177.382 QROCK = 0.000 QOUT = 8.716

TG = 357.000 MDOT = 0.0000

MFG = 0.01954082

MLS = 0.00000000

QIN = 179.867 QROCK = 358.642 QOUT = 0.545

TG = 327.069 MDOT = 0.0000

MFG = 0.01954083

MLS = 0.00000000

QIN = 195.934 QROCK = 379.947 QOUT = 5.958

TG = 298.423 MDOT = 0.0000

MFG = 0.01954084

MLS = 0.00000000

QIN = 199.419 QROCK = 401.253 QOUT = -1.207

TG = 270.572 MDOT = 0.0000

MFG = 0.01954086

MLS = 0.00000000

QIN = 110.188 QROCK = 0.000 QOUT = 4.550

TG = 244.321 MDOT = 0.0000

MFG = 0.01954086

MLS = 0.00000000

QIN = 110.863 QROCK = 221.932 QOUT = -0.105

TG = 218.963 MDOT = 0.0000

MFG = 0.01954087

MLS = 0.00000000

QIN = 112.602 QROCK = 0.000 QOUT = -3.689

TG = 194.888 MDOT = 0.0000

MFG = 0.01954087

MLS = 0.00000000

QIN = 115.349 QROCK = 243.237 QOUT = -6.270

TG = 172.637 MDOT = 0.0000

MFG = 0.01954089

MLS = 0.00000000

QIN = 118.514 QROCK = 253.890 QOUT = -8.432

TG = 152.581 MDOT = 0.0000

MFG = 0.01954089

MLS = 0.00000000

QIN = 125.927 QROCK = 0.000 QOUT = -6.344

TG = 134.945 MDOT = 0.0000

MFG = 0.01954089

MLS = 0.00000000

QIN = 74.925 QROCK = 137.598 QOUT = -4.535

TG = 119.260 MDOT = 0.0000

MFG = 0.01954093

MLS = 0.00000000

QIN = 65.703 QROCK = 142.924 QOUT = -5.785

TG = 105.043 MDOT = 0.0000

MFG = 0.01954096

MLS = 0.00000000

QIN = 69.639 QROCK = 148.251 QOUT = -4.486

TG = 92.320 MDOT = 0.0000

MFG = 0.01954098

MLS = 0.00000000

QIN = 63.660 QROCK = 0.000 QOUT = -13.129

TG = 80.781 MDOT = 0.0000

MFG = 0.01954100

MLS = 0.00000000

QIN = 67.260 QROCK = 158.903 QOUT = -12.193

TG = 71.617 MDOT = 0.0000

MFG = 0.02151672

MLS = 3.94267607

QIN = 73.539 QROCK = 164.230 QOUT = -8.576

TG = 64.479 MDOT = 0.0000

MFG = 0.02200834

MLS = 5.97348404

QIN = 32.749 QROCK = 84.778 QOUT = -9.642

TG = 58.692 MDOT = 0.0000

MFG = 0.02173183

MLS = 6.72945023

QIN = 32.668 QROCK = 87.441 QOUT = -11.053

TG = 54.378 MDOT = 0.0000

MFG = 0.02116495

MLS = 5.98273897

QIN = 24.955 QROCK = 0.000 QOUT = -20.097

TG = 51.620 MDOT = 0.0000

MFG = 0.02073966

MLS = 4.73253298

QIN = -159.560 QROCK = 0.000 QOUT = 6.349

TG = 50.383 MDOT = 0.0000

MFG = 0.02031104

MLS = 3.98458767

QIN = -55.032 QROCK = 0.000 QOUT = -7.471

TG = 50.000 MDOT = 0.0000

MFG = 0.01999777

MLS = 3.51408696

QIN = -0.103 QROCK = 0.000 QOUT = -3.481

TG = 50.000 MDOT = 0.0000

MFG = 0.01980893

MLS = 2.80270386

QIN = -0.103 QROCK = 0.000 QOUT = 0.000

TG = 50.000 MDOT = 0.0000

MFG = 0.01969640

MLS = 2.44401813

QIN = -0.103 QROCK = 0.000 QOUT = 0.000

TG = 50.000 MDOT = 0.0000

MFG = 0.01963010

MLS = 2.25252724

QIN = -0.103 QROCK = 0.000 QOUT = 0.000

TG = 50.000 MDOT = 0.0000

MFG = 0.01959149

MLS = 2.30907607

QIN = -0.103 QROCK = 0.000 QOUT = 0.000

TG = 50.000 MDOT = 0.0000

MFG = 0.01956925

MLS = 2.36562514

QIN = -0.103 QROCK = 0.000 QOUT = 0.000

TG = 50.000 MDOT = 0.0000

MFG = 0.01955658

MLS = 2.42217374

QIN = -0.103 QROCK = 0.000 QOUT = 0.000

TG = 50.000 MDOT = 0.0000

MFG = 0.01954943

MLS = 2.47872257

QIN = -0.103 QROCK = 0.000 QOUT = 0.000

TG = 50.000 MDOT = 0.0000

MFG = 0.01954544

MLS = 2.53527141

QIN = -0.103 QROCK = 0.000 QOUT = 0.000

TG = 50.000 MDOT = 0.0000

MFG = 0.01954325

MLS = 2.59182024

QIN = -0.103 QROCK = 0.000 QOUT = 0.000

REFERENCES

- Dean, A. John. 1985. *Lange's Handbook of Chemistry*. McGraw-Hill Book Company. 10-54
- Holman, J.P. 1986. *Heat Transfer*. McGraw-Hill Book Company. 158-179
- Kays, W. M. and M. E. Crawford. 1980. *Convective Heat and Mass Transfer*. McGraw-Hill Book Company.
- Risk Reduction Engineering Laboratory. 1993. "Accutech Pneumatic Fracturing Extraction and Hot Gas Injection, Phase I." *Applications Analysis Report*. U.S. Environmental Protection Agency, EPA/540/AR-93/509. 27-40
- Risk Reduction Engineering Laboratory. 1992/93. "Pneumatic Fracturing Extraction of Low-Permeable Vadose Zones." *Technology Evaluation Report*. U.S. Environmental Protection Agency, EPA/540/R-93/509. I: 5-20
- Schuring, John and Paul Chan. 1991. "Vadose Zone Contaminant Removal By Pneumatic Fracturing." *Final Report*. U.S. Geological Survey, Dept. of Interior, U.S.G.S. Award 14-08-0001-G1739.
- Schuring, John, Valdis Jurka and Paul Chan. 1991/92. "Pneumatic Fracturing to Remove VOC's." *Remediation Journal/Winter Report*. 51-68
- Shaw et al. 1991. "Catalytic Oxidation of Trichloroethylene and Methylene Chloride." *Emerging Technologies in Hazardous Waste Management III, ACS Symposium Series*. 518: 358-379
- Stasa, L. Frank. 1985. *Applied Finite Element Analysis for Engineers*. Holt, Rinehart and Winston. 421-425
- Stephenson, M. Richard and Stanislaw Malanowski. 1985. *Handbook of the Thermodynamics of Organic Compounds*. Elsevier Science Publishing Co., Inc. 1-292
- Thomas, C. Lindon. 1992. *Heat Transfer*. Prentice Hall, Inc. 188-247
- Thomas, C. Lindon. 1991. *Mass Transfer Supplement to Heat Transfer*. Prentice Hall, Inc. 108-154